Leghemoglobin is nitrated in functional legume nodules in a tyrosine residue within the heme cavity by a nitrite/ peroxide-dependent mechanism

Martha Sainz[1], Laura Calvo-Begueria[1], Carmen Pérez-Rontomé[1], Stefanie Wienkoop[2], Joaquín Abián[3], Christiana Staudinger[3], Silvina Bartesaghi[4,5], Rafael Radi[4] and Manuel Becana[1,*]

[1]Departamento de Nutrición Vegetal, Estación Experimental de Aula Dei, Consejo Superior de Investigaciones Científicas (CSIC), 50080 Zaragoza, Spain,

[2]Department of Ecogenomics and Systems Biology, University of Vienna, 1090 Vienna, Austria,

[3]Laboratorio de Proteómica CSIC-Universidad Autónoma de Barcelona, Instituto de Investigaciones Biomédicas de Barcelona, 08036 Barcelona, Spain,

[4]Departamento de Bioquímica and Center for Free Radical and Biomedical Research, and [5]Departamento de Educación Médica, Facultad de Medicina, Universidad de la República, Montevideo 11800, Uruguay

Received 12 December 2014

Corresponding author: Prof. Manuel Becana, Estación Experimental de Aula Dei, CSIC, Apartado 13034, 50080 Zaragoza, Spain. Phone: +34-976-716055. Fax: +34-976-716145.

*For correspondence (E-mail: becana@eead.csic.es).

Running title: Leghemoglobin tyrosine nitration

Keywords: *Glycine max*, leghemoglobin, legume nodules, nitrogen dioxide, peroxynitrite, *Phaseolus vulgaris*, protein tyrosine nitration.

Total word count (7765). Summary (244), Introduction (888), Results (1880), Discussion (1918), Experimental procedures (1823), Acknowledgements (116), Table titles (8), Figure legends (888).

Not included in total word count: References (1559).

Significance statement. We found that in functional legume nodules grown with or without nitrate, leghemoglobin, a crucial protein in symbiotic nitrogen fixation, is preferentially nitrated in a tyrosine within the heme pocket by a mechanism involving oxoferryl heme and nitrogen dioxide rather than peroxynitrite. Therefore, a low concentration of nitrated leghemoglobin is compatible with nodule activity, and we propose that leghemoglobins may act as a sink of toxic peroxynitrite and have a protective role in the symbiosis.

SUMMARY

Protein Tyr nitration is a post-translational modification yielding 3-nitrotyrosine (NO_2-Tyr). Formation of NO_2-Tyr is generally considered as a marker of nitroxidative stress and is involved in some human pathophysiological disorders, but it has been poorly studied in plants. Leghemoglobin (Lb) is an abundant hemeprotein of legume nodules that plays an essential role as O_2 transporter. Liquid chromatography coupled to tandem mass spectrometry was used for a targeted search and quantification of NO_2-Tyr in Lbs. For all Lbs examined, Tyr^{30}, located in the distal heme pocket, is the major target of nitration. Lower amounts were found for NO_2-Tyr^{25} and NO_2-Tyr^{133}. Nitrated Lb and other as yet unidentified nitrated proteins were also detected in nodules of plants not receiving NO_3^- and were found to decrease during senescence. This demonstrates formation of nitric oxide (•NO) and NO_2^- by alternative means to nitrate reductase, probably *via* a NO synthase-like enzyme, and strongly suggests that nitrated proteins perform biological functions and are not merely metabolic byproducts. *In vitro* assays with purified Lbs revealed that Tyr nitration requires $NO_2^- + H_2O_2$ and that peroxynitrite is not an efficient inducer of nitration, possibly by isomerizing it to NO_3^-. Nitrated Lb is formed *via* oxoferryl Lb, which generates nitrogen dioxide and tyrosyl radicals. This mechanism is distinctly different from that involved in heme nitration. Formation of NO_2-Tyr in Lbs is a consequence of active metabolism in functional nodules, where Lbs may act as a sink of toxic peroxynitrite and may play a protective role in the symbiosis.

INTRODUCTION

The molecular interaction of legumes and soil bacteria (rhizobia) culminates with the formation of nodules, generally on the roots. Legume nodules are unique symbiotic organs where atmospheric N_2 is reduced to ammonia assimilable for the plant in exchange for photosynthetically produced sugars. This biological N_2 fixation is highly beneficial for agriculture and the environment as it allows a reduction in the input of nitrogen fertilizers. Nodule function requires leghemoglobins (Lbs), hemeproteins that occur at concentrations of 1-5 mM in the cytosol of nodule host cells. These proteins transport and deliver O_2 to the symbiosomes at a low but steady concentration that allows efficient bacteroid respiration while preventing nitrogenase inactivation (Appleby and Bergersen, 1980). Generally, there are several Lb isoproteins in the nodules. Soybean nodules contain four major Lbs and bean nodules one major Lb (Fuchsman and Appleby, 1979).

Only the ferrous form of Lbs binds O_2 and under physiological conditions 20% of the ferrous Lb is oxygenated and 80% is deoxygenated. However, nonfunctional forms of Lb may be produced in nodules (Lee *et al.,* 1995) by redox reactions involving reactive oxygen species (ROS). Ferric Lb may be generated by autoxidation of oxygenated Lb, and ferryl Lb (Lb^{4+}=O, formally $oxoFe^{4+}$) by oxidation of ferrous or ferric Lbs with H_2O_2 (Aviram *et al.,* 1978; Moreau *et al.,* 1995). *In vitro* studies have shown that the oxidative attack of H_2O_2 on Lbs gives rise to protein radicals, which are then quenched *via* formation of intramolecular (heme-protein) and intermolecular (dimers) cross-links (Moreau *et al.,* 1995). Ferrous, ferric and ferryl Lbs can react also with reactive nitrogen species (RNS). Thus, ferrous Lb binds •NO avidly to form the nitrosyl complex (LbNO), which has been detected in intact nodules (Mathieu *et al.,* 1998; Meakin *et al.,* 2007). *In vitro* oxygenated ferrous Lb and ferric Lb are able to isomerize $ONOO^-$ to NO_3^- and ferryl Lb is reduced by nitric oxide (•NO) (Herold and Puppo, 2005a,b). Recently, we reported the presence in soybean nodules of green derivatives of Lbs having a nitro (NO_2) group on the 4-vinyl of the heme (nitri-heme) (Navascués *et al.,* 2012). By analogy with similar nitri-hemes found *in vitro* in myoglobin (Mb; Bondoc and Timkovich, 1989) and

hemoglobin (Hb; Otsuka *et al.,* 2010), and to avoid confusion with Lb nitrated in Tyr residues, we will refer to those Lbs as nitri-Lbs.

The nitration of Tyr residues in proteins involves the substitution of a H atom by a NO_2 group to yield NO_2-Tyr. This post-translational protein modification has attracted much attention in studies related to human health as it is involved in diverse pathological conditions (Schopfer *et al.,* 2003; Radi, 2004). Our knowledge of protein nitration is much more limited in plants, where an increase in the amount of nitrated proteins is associated to nitroxidative stress (Corpas *et al.,* 2007; Cecconi *et al.,* 2009; Begara-Morales *et al.,* 2013). Many of these studies are based on proteomic approaches, in which the proteins are separated in two-dimensional gels, detected with anti-NO_2-Tyr antibody, and identified (Chaki *et al.,* 2009; Galetskiy *et al.,* 2011; Begara-Morales *et al.,* 2013). In other cases, the plants are treated with •NO or $ONOO^-$ donors prior to proteomic analysis (Tanou *et al.,* 2012). Detailed studies using immunoprecipitation and/or semiquantitative assays with antibodies led to the identification of *o*-acetylserine(thiol)lyase (Álvarez *et al.,* 2011) and glutamine synthetase (Melo *et al.,* 2011) as targets of nitration. However, to our knowledge there are no studies showing unequivocally the presence and site of NO_2-Tyr residues in plant proteins *in vivo*. In an incisive work, Lozano-Juste *et al.* (2011) were able to detect a peptide of glyceraldehyde-3-phosphate dehydrogenase with an NH_2-Tyr residue, and concluded that this was generated by reduction of NO_2-Tyr during the mass spectrometry (MS)-based proteomic analysis, emphasizing that Tyr nitration analyses are prone to artifacts.

The major drawbacks for studying protein nitration *in vivo* are indeed the low abundance of nitrated proteins and the potential artifacts that may arise during processing and MS analysis of samples. Because Lb is essential for symbiotic N_2 fixation and participates in multiple reactions involving ROS and RNS, we reasoned that this hemeprotein might be a target of nitration *in vivo* and that its high abundance in nodules would facilitate the quantification of NO_2-Tyr by dedicated MS procedures. Further motivation for undertaking this research was the puzzling observation that nitri-Lbs have their apoproteins intact (Navascués *et al.,* 2012), which suggests that nitration of hemes and of Tyr residues, if any, should obbey distinct mechanisms and/or occur at different developmental stages and/or stress conditions of nodules.

In this work, we demonstrate that Lbs bearing NO_2-Tyr are present in legume nodules and that Tyr^{30}, which is located in the heme distal pocket, is the major target of nitration. Nitrated Lb decreases during nodule senescence and is present also in nodules of plants that were not given any NO_3^- in the nutrient solution. This indicates that there is a steady-state level of nitrated Lb *in vivo* and that sources other than bacteroid or plant nitrate reductases, probably a •NO synthase (NOS)-like activity, also produce the NO_2^- required for nitration. Based on *in vitro* assays that generate nitrating molecules, such as nitrogen dioxide radicals ($•NO_2$) and $ONOO^-$-derived species, we propose a mechanism entailing ferryl Lb and $•NO_2$, rather than $ONOO^-$, that accounts for the Tyr nitration pattern of Lb observed *in vivo*. Finally, we compare the mechanisms involved in heme and Tyr nitration and discuss their biological relevance.

RESULTS

Physiological state of nodules during natural and induced senescence

Two crop legumes, bean and soybean, were chosen to investigate Lb nitration because they have been extensively used by our group and others in studies of nodule natural and induced senescence (Pfeiffer *et al.,* 1983; Evans *et al.,* 1999; Escuredo *et al.,* 1996; Gogorcena *et al.,* 1997). Bean and soybean plants were grown in controlled-environment cabinets and under field conditions, respectively, and nodules were harvested at three developmental stages. Additional experiments were set up with bean plants grown in the complete absence of NO_3^- to compare nitration levels in nodules, as well as with bean plants treated with 10 mM NO_3^- for 4 days to induce senescence of young nodules. The total soluble protein and Lb of host cells are markers of the physiological state of nodules and were found to decrease by 19% and 39% in senescent bean nodules and by 27% and 20% in senescent soybean nodules; however, much larger decreases, 44% for soluble protein and 74% for Lb, were found in NO_3^--treated bean nodules (Figures 1a,b). The NO_2^- content of nodules was also determined as it is relevant for our nitration studies. Bean nodules contained very low amounts, ~5-8 nmol g^{-1} fresh wt (detection limit ~1 nmol g^{-1} fresh wt), whereas the NO_2^- content of soybean nodules reached ~40-80 nmol g^{-1} fresh wt, showing a decreasing trend with aging (Figure 1c).

The protein nitration profiles were examined on immunoblots with an anti-NO_2-Tyr antibody (Figure 2a,b). These allowed us to make a number of interesting observations. First, the nitration patterns of bean and soybean nodules were similar during senescence, and in fact nitrated proteins were virtually undetectable in aged or NO_3^--treated bean nodules and hardly visible in senescent soybean nodules. Second, nitration was more intense in soybean nodules (readily visible bands with 20 μg protein) than in bean nodules (requiring 50 μg protein). Third, nodules of bean plants not receiving NO_3^- had substantial nitration levels. Fourth, comparison of immunoblots and the respective Coomassie-stained gels revealed that a few proteins with lower abundance than Lb were intensely nitrated. These proteins were not identified and had apparent molecular masses of ~32, 38 and 45 kDa in bean nodules and ~28, 34, 38, 48 and 75 kDa in soybean nodules. Finally, nitrated Lb was hardly detectable on immunoblots of bean nodules and not visible on immunoblots of soybean nodules. To verify the presence of nitrated Lb in nodule extracts using immunoblots, a preparative native gel was loaded with high amounts (~500 μg) of protein and the bands corresponding to bean Lb*a* (PvLb*a*) and soybean Lb*a* and Lb*c* (GmLb*a* and GmLb*c*) were excised, eluted and analyzed on SDS-gels and immunoblots. This demonstrated that nitrated Lb is present in nodules (Figure 2b). Direct in-gel trypsinization of the excised Lb bands and subsequent MS analysis or direct analysis of crude nodule extracts by MS with Orbitrap technology also confirmed the presence of very low levels of nitrated Lb.

Nitration of Lbs occurs in legume nodules and decreases during senescence

The tryptic peptides of Lbs obtained as indicated above were independently analyzed by μLC-ESI-MS/MS and nLC-ESI-MS/MS with similar results. Both methods were used in order to increase the reproducibility and confidence of the identification and quantification of the very low abundant modified peptides. The use of dithiothreitol or β-mercaptoethanol was avoided to prevent reduction of NO_2-Tyr residues, which may be mediated by the hemeproteins themselves at 37°C and above (Balanbali *et al.,* 1999; Söderling *et al.,* 2007), as often practised in proteomic analyses. Because Lbs do not contain Cys residues, the alkylating reagent iodoacetamide was also omitted prior to trypsinization. An illustrative example is the tryptic peptide GNIPQYSVVFYTSILEK of PvLb*a* and its mononitrated species GNIPQY*SVVFYTSILEK (NO_2-Tyr^{25}) and

GNIPQYSVVFY*TSILEK (NO_2-Tyr^{30}). The three peptide species were fully resolved (Figure S1) and unequivocally identified by their MS/MS profiles (Figure 3). Likewise, we found in nodules the nitrated peptides ANIPQYSVVFY*TSILEK (NO_2-Tyr^{30}) of GmLb*a* and ANIPQYSVVFY*NSILEK (NO_2-Tyr^{30}) of GmLbc_1, as well as a small proportion (0.16-0.34%) of the C-terminal peptide AWEVAY*DELAAAIK (NO_2-Tyr^{133}) of GmLb*a*. We were unable to detect in nodules the dinitrated species NO_2-Tyr^{25} + NO_2-Tyr^{30} or mononitrated NO_2-Tyr^{133} in PvLb*a*, and the same occurred for mononitrated NO_2-Tyr^{25} in GmLb*a* and GmLbc_1.

LC-MS/MS aproaches based on targeted precursors and selected reaction monitoring (SRM) were used to determine the proportion of NO_2-Tyr^{30} in Lbs during natural and NO_3^--induced nodule senescence. We chose Tyr^{30} to quantify nitration because it is the most abundant nitrated Tyr residue and is important for Lb function (Kundu *et al.,* 2004). Figure 4 shows that young nodules contain 0.23% of nitrated PvLb*a*, 0.95% of nitrated GmLb*a* and 2.31% of nitrated GmLbc_1. Similar values of Lb nitration were obtained for nodules of plants than had received 0 or 0.25 mM NH_4NO_3 in the nutrient solution. The proportions of nitrated Lb relative to total Lb decreased during the natural (~30%) and NO_3^--induced (~60%) senescence of bean nodules as well as with advanced aging (~70%) of soybean nodules (Figure 4).

Nitration of Tyr residues *in vitro*: in search for a mechanism *in vivo*

The model structure of GmLb*a* shows that Tyr^{30} is located in the distal heme pocket, Tyr^{133} is also in the heme pocket but situated laterally, and Tyr^{25} is outside the heme crevice (Figure 5). Because Tyr^{30} is the main target of nitration *in vivo*, we surmised that the heme may participate in nitration of this Tyr residue. Considering that NO_2^- and •NO lack of sufficient reactivity to cause nitration but may give rise to the nitrating agents $•NO_2$ and $ONOO^-$ in the presence of H_2O_2 (Herold, 2004; Nicolis *et al.,* 2004), we assayed nitration using the estimated concentrations of ferric Lb (10 μM), H_2O_2 (20-100 μM) and NO_2^- (100 μM) in nodules or in other plant tissues (Evans *et al.,* 1999; Becana and Klucas, 1992). Also, care was taken to perform all the reactions at physiological conditions of nodules (pH 6.5 and 26°C) rather than at conditions commonly used for animal systems (pH 7.4 and 37°C). At proportions of Lb:H_2O_2:NO_2^- of 1:2:2 and 1:2:10, nitration was less intense than at 1:10:10 or 1:10:100. The two last proportions were

chosen for further studies because the high yields of the nitrated products facilitated their separation on preparative gels and the subsequent MS analyses (see below). Treatment of 10 μM of PvLb*a* or GmLb*a* with 100 μM H_2O_2 + 100 μM NO_2^- yielded 25-50% NO_2-Tyr^{30} and ~0.5% NO_2-Tyr^{25} (except for GmLbc_1, which produced 13.5% NO_2-Tyr^{25}) (Table 1). Increasing NO_2^- concentration to 1 mM, while keeping H_2O_2 constant, produced ~70% of NO_2-Tyr^{30} and 0.4-1.4% NO_2-Tyr^{25} (Table 1). Thus, NO_2-Tyr^{30} was the preferred target of Lb nitration by H_2O_2 + NO_2^- *in vitro*.

To gain further insights on the mechanism of the nitration reaction, Lbs were treated with H_2O_2 + NO_2^- in the presence of potential inhibitors (Bartesaghi *et al.,* 2004, 2006; Castro *et al.,* 2004) and the products were analyzed on immunoblots (Figure 6a). These show that nitration does not take place when H_2O_2 was omitted and that the reaction was inhibited by deferoxamine mesylate (DFO; powerful Fe^{3+}chelator and •NO_2 scavenger), 4-hydroxyphenylacetic acid (pHPA; hydrophylic structural analog of Tyr that intercepts •NO_2), uric acid (scavenger of radicals derived from $ONOO^-$) and cyanide (ligand of ferric hemeproteins). The addition of diethylenetriamine-pentaacetic acid (DTPA; metal ion chelator) had no effect. We then examined whether $ONOO^-$ could be also a nitrating agent in our system by treating Lbs with 3-mopholino-sydnonimine (SIN-1) (Figure 6b) or with synthetic $ONOO^-$ (Figure 6c) in the presence of 100 μM DTPA to suppress metal-catalyzed nitration. It has been shown that SIN-1 generates nearly equimolar amounts of •NO and superoxide radicals (O_2^-•), which then react with each other producing a flux of $ONOO^-$ for at least 2 h (Álvarez *et al.,* 2002). At pH 6.5 and 26°C, we could only detect weak nitration on immunoblots when 10 μM of GmLb*a* or PvLb*a* were treated with 1 mM SIN-1 for 1 h (6 μg protein) or for 2 h (3 μg protein) (Figure 6b). Nitration was not visible when 1 mM SIN-1 was applied for 1 h and 3 μg of Lb was loaded. Nevertheless, significant nitration occurred when the pH was raised to 7.4 and the temperature to 37°C. To further support the absence of nitration at relevant conditions for nodule cells, Lbs were exposed to pure $ONOO^-$ in the presence of a physiological concentration of CO_2 (5 mM HCO_3^- at pH 6.5) because CO_2 potentiates the nitrating effect of $ONOO^-$ (Gow *et al.,* 1996). We could detect significant nitration only when 30 μM Lb was treated with a bolus of 500 μM $ONOO^-$ and 6 μg protein was loaded on the gels, and nitration was negligible when 60 μM Lb and 3 μg protein were used (Figure 6c). Interestingly, in contrast with the SIN-1 treatment, which produces a controlled flux of $ONOO^-$ over time,

only Lb aggregates could be observed with the bolus addition of pure $ONOO^-$ (Figure 6c).

Nitration of Tyr residues *in vitro* at preparative scale

The nitration reaction was scaled up using 1 mM Lb and proportions of Lb: H_2O_2: NO_2^- of 1:10:10 and 1:10:100. The resulting Lb derivatives were resolved on preparative native gels (Figure 7a). PvLb*a* and GmLba yielded three major products (B1-B3 and S1-S3) when nitration was performed with 10 mM H_2O_2 + 10 mM NO_2^-. The same Lbs produced four major derivatives (B4-B7 and S4-S7) upon nitration with 10 mM H_2O_2 + 100 mM NO_2^-. Some of these protein derivatives are green, indicating modification of the hemes. Because our results showed formation of nitrating species during the reactions, we searched for the presence of nitrated hemes. These can be identified by MS as they have molecular ions of *m/z* 661 (616 + 45 Da), corresponding to replacement of a H by a NO_2 group. Tandem MS revealed that the *m/z* 661 ion exhibits a fragmentation pattern identical to that of the nitri-heme (Figure S2), suggesting that the NO_2 is also on a vinyl group (Navascués *et al.,* 2012). This peak was clearly detectable in proteins B1-B3 (red), B4 (green), S2 (red) and S3 (green). Therefore, the nitrated heme in those red proteins is at low levels, and the proteins B5-B7 (green) and S4-S7 (green), with virtually no peak at 661 Da, have other types of modified hemes as a result of the oxidative attack by H_2O_2.

All the proteins were eluted from the gels and analyzed by immunoblots, low-resolution MS (MALDI-TOF/TOF-MS) and high-resolution MS (Orbitrap nESI-FT-MS). Immunoblot (Figure 7b) and MS (Table S1) analyses revealed that each protein band contains NO_2-Tyr and is a mixture of monomers, dimers and in some cases trimers (B1, B4, S1 and S4), with molecular masses in the range of ~15300-15600, ~30500-31900 and ~46400-47900 Da, respectively. High-resolution MS analysis (± 0.2 Da) of the monomers (Table S1) confirmed the presence of NO_2-Tyr (+45 Da) in most of the proteins, as well as dinitration (+90 Da) in B4. It also revealed changes in the monoisotopic molecular masses of the monomeric proteins compared with the control proteins (15479 for PvLb*a* and 15233 for GmLb*a*). These changes are +13 Da for B1 and -190 Da for B5, B6 and B7, but were not investigated further as their relevance *in vivo* is uncertain.

DISCUSSION

Legume nodule senescence is characterized by, among other factors, a decline in N_2 fixation, soluble protein and Lb (for reviews see Puppo *et al.,* 2005; Becana *et al.,* 2010). Indeed, we confirmed the senescent stage of nodules harvested from fruiting plants or from young plants supplied with NO_3^- because the total soluble protein and Lb of bean and soybean nodules decreased markedly due to an increase in endoprotease activity (Pfeiffer *et al.,* 1983; Pladys *et al.,* 1988). In particular, treatment of bean plants with 10 mM NO_3^- for 4 days caused a major decrease of Lb and Lb/soluble protein ratio (from 16% to 7%), indicating that Lb is especially prone to degradation (Figures 1a,b). This is consistent with an early observation that proteolytic activity against Lb is augmented at the acid pH of senescent nodules (Pladys *et al.,* 1988).

Bean nodules contained low amounts of NO_2^- but soybean nodules accumulated relatively high levels of this metabolite (Figure 1c). This is readily explained by the fact that bean nodule bacteroids (strain 3622) do not express nitrate reductase, whereas soybean nodule bacteroids (strain USDA110) display relatively high nitrate reductase activity, which is responsible for most NO_2^- produced in soybean nodules (Becana *et al.,* 1989; Meakin *et al.,* 2007). This NO_2^- accumulation may, in fact, be a contributing factor to the high nitration levels of soybean nodules relative to bean nodules (Figure 2a). However, nitration was clearly detectable in bean nodules that had not received any NO_3^- (Figure 2a), evidencing that alternative sources to bacteroid and plant nitrate reductases also exist in nodules to generate •NO and/or the NO_2^- derived therefrom. In fact, •NO and NO_2^- are precursors of nitrating RNS and the presence of the LbNO complex has been reported in soybean nodules grown without NO_3^- (Mathieu *et al.,* 1998). A likely source of RNS is a NOS-like activity. In plants, this activity was originally described in lupin (*Lupinus albus*) roots and nodules and measured by the conversion of ^{14}C-Arg into ^{14}C-citrulline at a rate of 150-200 pmol •NO produced min^{-1} mg^{-1} protein (Cueto *et al.,* 1996). We have observed similar values in bean nodules with a highly sensitive and specific

assay in which •NO was detected by ozone chemiluminiscence (Corpas *et al.,* 2007). Together, these observations give strong support to the presence of NOS-like activity in legume nodules.

The accumulation of nitrated proteins is assumed to be a marker of nitroxidative stress in animals (Schopfer *et al.,* 2003; Radi, 2004) and plants (Corpas *et al.,* 2007). Our finding that protein nitration decreases with nodule senescence was completely unexpected as nitrated proteins may accumulate during aging of leaves and roots of several plants, including legumes (Begara-Morales *et al.,* 2013). At present we cannot offer an explanation for this other than it may be a feature of nodules and/or that nitrated proteins are preferential substrates for the nodule proteases induced during senescence. Consistent with this decreasing trend for nitrated proteins of nodules in general, we demonstrate here that Lb nitration occurs *in vivo* and is more intense in young than in senescent nodules (Figure 4). We had anticipated that Lb may be prone to nitration in nodules because it reacts rapidly *in vitro* with ROS and RNS (Becana and Klucas, 1992; Moreau *et al.,* 1995, 1996). However, other still unknown proteins appear to be more nitrated than Lb, for they exhibit intense bands on immunoblots and are considerably less abundant than Lb. Our data also show that a steady-state level of nitrated Lb, roughly estimated in the range of 0.1-1%, occurs as a result of normal nodule metabolism. A few unindentified nitrated proteins have been detected also by immunoblots in other 'control' (unstressed, young) plant tissues (Chaki *et al.,* 2011; Galetskyi *et al.,* 2011; Tanou *et al.,* 2012; Begara-Morales *et al.,* 2013). Thus, the existence of a basal nitration level is a general phenomenon, strongly suggesting that nitrated proteins perform biological functions and are not merely metabolic byproducts.

Previous findings of oxidative damage of crucial biomolecules (Evans *et al.,* 1999) and production of nitri-Lbs (Navascués *et al.,* 2012) in senescing soybean nodules indicate that nitroxidative stress occurs at very late stages of senescence. We are therefore bound to conclude that NO_2-Tyr in proteins is not a useful marker of nitroxidative stress, at least in nodules. Also, the decreased content of nitrated Lbs in senescing tissue strongly suggests that the two forms reported so far of modified Lbs, nitri-hemes and nitrated apoproteins, are generated by distinct mechanisms, as we will discuss below.

The mechanism of Tyr nitration in Lbs was investigated. Essentially, three types of mechanisms have been proposed for Tyr nitration of animal globins (Figure 8). (*a*)

Formation of ferryl globins and their radical forms, which oxidize NO_2^- to $\bullet NO_2$ (Figure 8a; Van der Vliet *et al.,* 1997; Herold, 2004; Sakamoto *et al.,* 2004). (*b*) Fenton reaction, catalyzed by traces of free or protein-associated transition metals, in which the resulting •OH oxidizes NO_2^- to $\bullet NO_2$ (Figure 8b; Thomas *et al.,* 2002). (*c*) Formation of $ONOO^-$ or its derived species, peroxynitrous acid (ONOOH) and nitrosoperoxocarboxylate ($ONOOCO_2^-$), which may undergo homolytic cleavage to •OH, $\bullet NO_2$ and carbonate radical ($CO_3^{-\bullet}$) (Figure 8c; Radi, 2004; Bartesaghi *et al.,* 2004, 2006). Mechanisms (a) and (b) require $NO_2^- + H_2O_2$, whereas mechanism (c) does not. In our experiments with Lb, the failure of DTPA to inhibit Tyr nitration rules out mechanism (b). However, $ONOO^-$ might be formed *via* $\bullet NO + O_2^{-\bullet}$ (Radi, 2004), and this possibility was examined by treating Lbs with the $ONOO^-$-generating compound SIN-1 or with synthetic $ONOO^-$. In both cases, we found no significant nitration when the reactions were carried out at pH 6.5 and 26°C, physiological conditions of nodules (Pladys *et al.,* 1988). Instead, we did detect nitration when a high flux of $ONOO^-$ was generated from SIN-1 at pH 7.4 and 37°C for 2 h. Under these conditions, the production and stability of $ONOO^-$ are higher and thus 1 mM SIN-1 generates an accumulated level equivalent to ~0.5 mM $ONOO^-$ in 1 h (Álvarez *et al.,* 2002). This is an extremely high amount, unlikely to be produced in healthy plant tissues and certainly not in young, actively N_2-fixing nodules. Taking into account that 500 μM of pure $ONOO^-$ does not cause appreciable nitration of Lb and that the pH of nodules decreases from 6.5 to 5.5 during nodule senescence, we conclude that direct nitration of Lb by $ONOO^-$ is probably irrelevant *in vivo*, although we cannot entirely preclude the possibility that some minor nitration occurs *via* $ONOO^-$. This conclusion is consistent with previous *in vitro* studies showing that horse Mb and human Hb catalyze $ONOO^-$ isomerization without being significantly nitrated (Herold and Shivashankar, 2003).

The inhibition of nitration by DFO, pHPA and uric acid (Figure 6a), which preferentially scavenge $\bullet NO_2$ (Bartesaghi *et al.,* 2004, 2006; Castro *et al.,* 2004), supports mechanism (a). Interestingly, DFO suppressed formation of dimers and other aggregates and decreased nitration of monomeric Lb, consistent with previous work showing that DFO inhibits dimerization and nitration of free Tyr by mechanisms that are independent of metal ions (Bartesaghi *et al.,* 2004). In sharp contrast, cyanide completely inhibited nitration of the monomer, indicating the participation of the heme in the reaction.

However, it did not inhibit dimerization, which may be attributed to side reactions of cyanide-derived radicals (Castro *et al.,* 2004).

Studies of Tyr nitration of Mb and Hb with NO_2^- + H_2O_2 have led to the proposal that the nitrating compound is •NO_2 and/or heme-bound $ONOO^-$, depending of the relative concentrations of NO_2^- and H_2O_2 (Herold, 2004; Nicolis *et al.,* 2004). Moreover, in all cases, a tyrosyl radical (•Tyr) must be formed from Tyr, a reaction that cannot be achieved by $ONOO^-$ *per se* (Castro *et al.,* 2004; Radi, 2004). We conclude that Tyr nitration of Lb occurs by mechanism (a), requiring ferryl Lb to generate both •NO_2 and •Tyr, which then recombine to form NO_2-Tyr (Figure 8a). The inhibition of Lb nitration by cyanide further supports a ferryl-mediated, heme-dependent mechanism. This would explain why Tyr^{30}, located in the distal heme pocket, is a preferred target for *in vivo* and *in vitro* nitration. However, the oxidation of Tyr^{30} by the oxoferryl intermediate is unlikely to be direct because the distance between the two structures is >7 Å (Figure 5b,c). Generally, Tyr residues with at least one carbon within 4-5 Å from the oxoferryl are assumed to be amenable for their direct one-electron oxidation to •Tyr (Prasad *et al.,* 2007). Thus, in the case of Lb, Tyr^{30} oxidation may be mediated *via* intramolecular electron transfer (Petruk *et al.,* 2012). Formation of •Tyr must also occur on Tyr^{25} and Tyr^{133}, as they were found to be nitrated. Notably, a protein radical was detected by EPR in GmLb*a* treated with H_2O_2 in the absence of NO_2^-, and the signal was assigned to Tyr^{133} (Moreau *et al.,* 1996). This observation is not at odds with our results, considering that ferryl Lb is responsible for the H abstraction from Tyr according to mechanism (a).

The nitrated Lbs described here are different from nitri-Lbs (Navascués *et al.,* 2012). Nitrated Lbs contain NO_2-Tyr whereas nitri-Lbs do not, probably as a result of the different free radical mediated reactions implicated in their production. Formation of nitrated Lbs requires H_2O_2 to generate ferryl Lb and ultimately •Tyr, whereas formation of nitri-Lbs requires very high NO_2^- concentrations but not H_2O_2, and involves HNO_2 as precursor of the nitrating agent. Treatment of Lbs with NO_2^- + H_2O_2 elicited not only Tyr nitration but also heme modifications and protein dimerization and aggregation, as shown by immunoblots (Figure 7b) and MS analysis (Table S1). These Lb derivatives are originated by intermolecular reactions of protein radicals, not necessarily entailing •Tyr. Notably, the dimers and aggregates contain high amounts of NO_2-Tyr relative to monomers. In this respect, we noted that $ONOO^-$ also produced aggregates of nitrated Lb,

whereas SIN-1 formed mainly monomers (Figures 6b,c). We attribute this to differences in the concentrations of •Tyr achieved with the different modes of exposure, which are much greater with the bolus addition of $ONOO^-$ than with SIN-1. Thus, in the first case, •Tyr radicals are more likely to recombine forming Tyr-Tyr bridges than with SIN-1.

The relative abundance of the two types of modified Lbs during nodule aging is also different. The content of nitrated Lbs is higher in young (very active) nodules, which evidences the production *in vivo* of ferryl Lb, $•NO_2$ and •Tyr. Nitration of Tyr^{30} may interfere with Lb function because this amino acid residue allows for a proper delivery of O_2 (Kundu *et al.,* 2004). Our results show that a low steady-state level of nitrated Lbs is fully compatible with nodule activity and that Lb is nitrated by a mechanism involving oxyferryl heme rather than $ONOO^-$, most likely as a result of the efficient capacity of Lb to isomerize $ONOO^-$ to NO_3^- (Herold and Puppo, 2005a). Taking these results together with other *in vivo* observations (Mathieu *et al.,* 1998; Navascués *et al.,* 2012), we propose that, in young nodules, Lbs may act as a sink of •NO and derived RNS such as $ONOO^-$ to keep the symbiosis active, preventing rejection of, or toxic effects on, the bacteroids. By contrast, the content of nitri-Lbs is higher in old (less active or inactive) nodules and may be a result of an excessive production of RNS associated to senescence and nitroxidative stress. Further work will be needed to determine if Lb dimers and other aggregates occur *in vivo* during legume nodule development and senescence.

EXPERIMENTAL PROCEDURES

Plant growth

Bean (*Phaseolus vulgaris* L. cv Contender) was inoculated with *Rhizobium leguminosarum* bv *phaseoli* strain 3622 and grown in vermiculite-containing pots under controlled environment conditions (Gogorcena *et al.,* 1997) with either 0 or 0.25 mM NH_4NO_3 in the nutrient solution. This low NH_4NO_3 concentration stimulates nodulation of most legumes. Young, mature and senescent nodules were harvested from beans of ~1 month (vegetative stage), ~1.5 months (flowering stage) and ~2 months (fruiting stage), respectively. In another set of experiments, beans of ~1 month were supplied with 10 mM KNO_3 for 4 days to induce nodule senescence. Soybean (*Glycine max* Merr. cv Williams)

was inoculated with *Bradyrhizobium japonicum* strain USDA110 and grown in an experimental plot in Sevilla (Spain) from July to September. Young, mature and senescent nodules were harvested from soybeans of ~1 month (vegetative stage), ~2 months (late flowering-early fruiting stage) and ~3 months (fruiting stage), respectively. Bean and soybean nodules were frozen in liquid nitrogen and stored at -80°C.

Physiological state and immunoblot analyses of nodules

Total soluble protein and Lb were used as markers of the physiological state of nodules (Pfeiffer *et al.,* 1983; Escuredo *et al.,* 1996). Nodules (200 mg) were homogenized with 2 x 500 μl 20 mM potassium phosphate (pH 7.0), and the extracts were cleared by centrifugation (20000 ***g***, 20 min). Soluble protein was determined by the dye-binding microassay (Bio-Rad; http://www.bio-rad.com) using bovine serum albumin as a standard. Lb concentration was determined by the alkaline pyridine method, based on the differential spectra of the dithionite-reduced *versus* ferricyanide-oxidized pyridine-hemochromes (556 nm *minus* 539 nm, extinction coefficient 23.4 mM^{-1} cm^{-1}; Appleby and Bergersen, 1980).

Some biochemical markers relevant to our nitration studies, including NO_2^- concentrations and protein nitration profiles, were also determined in nodules. Nitrite was quantified by diazotization after rapid and complete deproteinization of nodule extracts (Becana *et al.,* 1989; Arrese-Igor *et al.,* 1998). Nodules (0.5 g) were ground in a mortar on melting ice with 5 ml of 1 M zinc acetate at 0°C. The precipitated proteins were removed by centrifugation and the supernatant mixed with an equal volume of ice-cold ethanol. After centrifugation, 500 μl of the clean extract was mixed with equal volumes of 1% sulfanilamide in 1.5 M HCl and 0.1% *N*-(1-naphthyl)-ethylenediamine dihydrochloride. Blanks containing sample but 1.5 M HCl instead of sulfanilamide were run in parallel. After 20 min at room temperature, the absorbance at 540 nm was read and NO_2^- concentration calculated with a calibration curve (0-20 nmol).

The protein nitration profiles of nodules were obtained using immunoblots. Nodule extracts, SDS-gels and transfer of proteins to polyvinylidene difluoride membranes (FluoroTrans; Pall, http://www.pall.com) were performed following standard protocols, but omitting reductants in the sample buffer. Membranes were probed with a monoclonal anti-NO_2-Tyr (Cayman, https://www.caymanchem.com) antibody and in some cases with a

polyclonal affinity-purified anti-Lb antibody (see below), both at a dilution of 1:1000. The secondary antibodies were, respectively, goat anti-mouse IgG (Bio-Rad) and goat anti-rabbit IgG (Sigma, http://www.sigmaaldrich.com) peroxidase conjugates, which were used at a dilution of 1:20000. Immunoreactive proteins were detected by chemiluminescence using the SuperSignal West Pico kit (Pierce, http://www.piercenet.com).

The antiserum against PvLb*a* was produced by injecting ~0.8 mg of protein in each of two white rabbits and was used to purify polyclonal monospecific antibodies by chromatography in CNBr-activated Sepharose 4 Fast Flow (GE Healthcare, www.gelifesciences.com). The immunoaffinity column was prepared with ~5 mg of protein. Conventional protocols for immunization and antibody purification were carried out by BioGenes (http://www.biogenes.de).

LC-MS/MS

For the identification and quantification of NO_2-Tyr in Lbs *in vivo*, nodules (200 mg) were ground in a ice-cold mortar with a medium (400 µl) consisting of 50 mM Tris-HCl (pH 8.0), 0.5 mM EDTA, 1% polyvinylpyrrolidone-10 and protease inhibitor cocktail (Complete Mini; Roche, https://lifescience.roche.com/shop/home). Extracts were centrifuged (13000 ***g***, 10 min) and the soluble proteins subjected to preparative native gel electrophoresis (12.5% acrylamide, 3 mm thick). Samples (400-500 µg of protein per lane) were mixed 1:4 (vol:vol) with loading buffer omitting SDS and reductants. Gels were run at 100 V for 2 h 15 min on a MGV-100 apparatus (CBS, http://www.cbsscientific.com). The bands of PvLba, GmLb*a* and GmLb*c* were carefully excised from the gels, cut into small pieces and kept at -20°C until MS analysis, which usually took place one week later. In-gel digestion was performed with trypsin at 37°C for 8 h with an automatic device (DigestPro MS; Intavis, http://www.intavis.com). For some MS experiments, proteins were eluted overnight with 10 mM NH_4HCO_3 with identical results.

Two types of analyses were used to detect and quantify the low abundant nitrated peptides of Lbs. The first analysis involved liquid chromatography coupled to tandem MS with micro-electrospray ionization (µLC-ESI-MS/MS). In this case, the instrument was an LTQ Velos (Thermo Scientific; www.thermofisher.com). Aliquots of the tryptic digest were diluted to 20 µl with 5% methanol and 1% formic acid and loaded onto a

chromatographic system consisting of a C_{18} preconcentration cartridge (Agilent Technologies; http://www.agilent.com) connected to a C_{18} tip column (15 cm x 150 μm, 5 μm; Nikkyo Technos, http://www.nikkyo-tec.co.jp). The separation was performed using a 40-min acetonitrile gradient from 3% to 40% (solvent A: 0.1% formic acid; solvent B: acetonitrile + 1% formic acid) at a flow rate of 1.0 μl min^{-1}. The HPLC system comprised an Agilent 1200 capillary pump, a binary pump, a thermostatted micro-injector and a micro-switch valve. The MS/MS system was operated in the positive ion mode with a spray voltage of 2 kV. Initial identification of the non-nitrated and nitrated peptides in the chromatograms was carried out in the data dependent mode, acquiring a full scan followed by ten MS/MS scans of the ten most intense signals detected in the MS scan. An exclusion time of 30 s was included to avoid repetitive MS/MS analysis of the dominant MS signals. Peptides were identified by database search of the MS/MS spectra using SEQUEST (Proteome Discoverer 1.3; Thermo Scientific). Search was performed with the following parameters: peptide mass tolerance 5 ppm, fragment tolerance 0.8 Da, enzyme set as trypsin, allowance up to two missed cleavages, and dynamic modification for Met oxidation (+15.995 Da) and Tyr nitration (+44.985 Da). Relative quantification was carried out using SRM. The areas of the signals of the product ions were integrated and the ratios of the areas of the modified to unmodified peptides were calculated. The transitions used to integrate the peak areas are given in Table S2.

For the second analysis, peptide digests were applied to an EASY-Spray PepMap RSLC C_{18} column (15 cm x 50 μm; particle size, 2 μm; Thermo Scientific) coupled to a one-dimensional nano-flow LC (Dionex UltiMate 3000; Thermo Scientific). The peptides were separated using a 60-min acetonitrile gradient from 95% of solvent A (0.1% formic acid) to 50% of solvent B (50% acetonitrile + 0.1% formic acid) at a flow rate of 300 nl min^{-1}. The nLC-ESI-MS/MS analysis was performed on a LTQ Orbitrap Elite (Thermo Scientific) at a resolution of 60,000. The repeat count was set to 1, repeat duration 20 sec, exclusion list size 500, exclusion duration 60 sec and exclusion mass width 10 ppm. Charge state screening was enabled with rejection of unassigned and 1+ charge states. Minimum signal threshold counts were set to 5,000. Peptide identification was carried out with SEQUEST as indicated for the first method. ProtMAX software was used for relative quantification of the identified nitrated peptides with respect to the unmodified ones by the relative abundances calculated from automated extraction of the summed ion

intensities of the targeted peptide precursor masses (Egelhofer *et al.,* 2013).

For both analyses, the monitored tryptic peptides with UniProt accession numbers of the proteins are given in Table S2.

Purification of Lbs and *in vitro* nitration

For *in vitro* nitration experiments, bean and soybean Lbs were purified essentially as described (Jun *et al.,* 1994). Nodule extracts were prepared in 50 mM Tris-HCl (pH 7.5), containing 1 mM EDTA and protease inhibitor cocktail. The protein was fractionated with 50-85% ammonium sulfate, resuspended in 10 mM Tris-HCl (pH 9.2), and oxidized with excess ferricyanide. The protein was dialyzed overnight with 50 mM potassium phosphate (pH 7.0), and applied to a hydroxyapatite column (HTP; Bio-Rad). The column effluent was concentrated and the buffer exchanged to 20 mM Tris-HCl (pH 8.0) with Vivaspin devices (10 kDa cutoff; Sartorius, http://www.sartorius.de). The protein was loaded onto a weak anion-exchange column (Whatman DE-52 cellulose; GE Healthcare) equilibrated with 20 mM Tris-HCl (pH 8.0). PvLb*a* was eluted with 80 mM NaCl in buffer, GmLb*a* with buffer alone, and GmLb*c* (Lbc_1 + Lbc_2 + Lbc_3) with a gradient of 0-100 mM NaCl in buffer.

Nitration of pure Lbs at analytical (10 μM ferric Lb) and preparative (1 mM ferric Lb) scales was conducted with relative proportions of Lb: H_2O_2: NO_2^- of 1:10:10 and 1:10:100. The assays were carried out in 20 mM potassium phosphate buffer (pH 6.5) at 26°C for 30 min. The proteins were then immediately loaded on SDS-gels and immunoblots performed with anti-NO_2-Tyr and anti-Lb antibodies. At the analytical scale, the effects of some compounds on nitration were tested by adding them in the reaction mix after Lb, but prior to NO_2^- + H_2O_2, at the following concentrations: DTPA (100 μM), DFO (100 μM), pHPA (5 mM), uric acid (10 μM) and KCN (10 mM). Nitration of Lbs was also attempted by exposing the proteins to SIN-1 (0.2-1 mM) for 1-2 h or to synthetic $ONOO^-$ (100-500 μM) for 5 min, at pH 6.5 and 26°C. For comparison, additional assays were performed by exposing Lbs to SIN-1 at pH 7.4 and 37°C for 1-2 h. Synthetic $ONOO^-$ was prepared by the reaction between H_2O_2 and NO_2^- at acid pH following standard protocols (Gow *et al.,* 1996; Bartesaghi *et al.,* 2006). The $ONOO^-$ preparations had <20% NO_2^- contamination but were free of H_2O_2. Any possible effect of contaminating NO_2^- was ruled out by control experiments with decomposed $ONOO^-$

('reverse-order addition'; Bartesaghi *et al.,* 2004).

At the preparative scale, the Lb nitration products were excised from gels, eluted with 10 mM NH_4HCO_3 and analyzed by MS to determine molecular masses of the holoproteins and hemes and to quantify NO_2-Tyr. Low-resolution MS was performed using different dilutions of the samples in 0.1% trifluoroacetic acid. The samples were spotted on a MALDI plate with sinapinic acid and analyzed using a MALDI-TOF/TOF mass spectrometer (4800 TOF/TOF; AB Sciex, http://www.absciex.com). High-resolution MS was performed by nLC-ESI-MS/MS with an LTQ XL-Orbitrap mass spectrometer (Thermo Scientific). For nESI-FT-MS analysis, 5 μl of sample diluted in 50% MeOH + 0.1% trifluoroacetic acid was loaded in the nanospray needle. Full MS spectra were acquired (50 microscans/sec) at a resolution of 100,000 using an energy on source of 35 (full range of *m/z* 300-1800). For heme analyses, the signals at *m/z* 616 and 661 were selected as precursor masses and product ion spectra were obtained by collision induced dissociation (isolation width 2.5 and collision energy 35). Spectra were deconvoluted using the Xtract tool included in the Xcalibur 2.0 software (Thermo Scientific).

ACKNOWLEDGMENTS

We thank Javier Luque (Universidad de Barcelona) for his invaluable help with Figure 5. M.S. was the recipient of a predoctoral contract (Programa Junta de Ampliación de Estudios) from CSIC. L.C.-B. was the recipient of a predoctoral contract (Formación de Personal Investigador) from Ministerio de Economía y Competitividad (MINECO). C.S. was funded by the Austrian Fonds zur Förderung der wis-senschaftlichen Forschung (P23441-B20). This work was mainly supported by MINECO-Fondo Europeo de Desarrollo Regional (AGL2011-24524 and AGL2014-53717-R) and CSIC (Proyecto Intramural Especial 201240E150). Additional funding was provided by grants of Agencia Nacional de Investigación e Innovación (Fondo Clemente Estable, FCE 6605) to S.B. and Universidad de la República and National Institutes of Health (RO1 AI095173) to R.R.

SUPPORTING INFORMATION

Additional Supporting Information may be found in the online version of this article.

Figure S1. Peak-base separation of non-nitrated and mono-nitrated peptides of PvLb*a*.

Figure S2. Tandem MS analyses of the molecular ions (*m/z* 661) of nitrated hemes.
(a) Fragmentation profile of heme from the green Lb derivative S6 (terminology according to Figure 7).
(b) Fragmentation profile of nitri-heme (Navascués *et al.,* 2012). Insets are close-up views of the spectra (range *m/z* ~480-660).

Table S1. Compilation of data obtained for Lb derivatives using immunoblots, low-resolution MS and high-resolution MS.

Table S2. MS/MS Transitions monitored for the calculation of the nitration ratios.

FIGURE LEGENDS

Figure 1. Physiological state of bean and soybean nodules.
Nodule contents of total soluble protein (a), Lb (b) and NO_2^- (c) during natural and NO_3^--induced senescence. The NO_2^- content of bean nodules was ~5-8 nmol g^{-1} fresh wt, close to the detection limit of the assay, and therefore it was not shown in the figure. Y, young nodules; M, mature nodules; S, senescent nodules; 4N, young nodules after 4 days of NO_3^- treatment. Data are means ± SE of four to six biological replicates. Means denoted by the same letter do not significantly differ at $P<0.05$ based on the Duncan's multiple range test.

Figure 2. Immunoblots showing the presence of nitrated proteins in bean and soybean nodules.
(a) Bean plants were grown in the absence of NO_3^- or under common conditions with 0.25 mM NH_4NO_3, and soybean plants were grown in the field. Nodule extracts were analyzed on 12.5% SDS-gels. Immunoblots *(up)* and Coomassie-stained gels *(down)* are shown. Protein loaded was 50 μg (bean) or 20 μg (soybean) per lane.

(b) Extracts from similar nodule samples as above were loaded on preparative native gels, then Lb bands were eluted and proteins were resolved on 15% SDS-gels and blotted. Protein loaded was 20 μg per lane.

Y, young nodules; M, mature nodules; S, senescent nodules; 4N, young nodules after 4 days of NO_3^- treatment. Molecular mass (kDa) markers are indicated on the left. Nitrated protein bands and nitrated Lb bands are marked with arrowheads and arrows, respectively. Immunoblots are representative of six (a) or three (b) blots obtained with different nodule samples, except that in a few cases nitration intensity was similar in Y and M nodules of bean plants grown on 0.25 mM NH_4NO_3.

Figure 3. Identification of nitrated peptides.

Fragmentation spectra of the unmodified GNIPQYSVVFYTSILEK peptide *(up)* of PvLb*a* and of its NO_2-Tyr^{25} *(centre)* and NO_2-Tyr^{30} *(down)* modified forms. The spectra were obtained with the LTQ Velos system on a data-dependent mode.

Figure 4. *In vivo* nitration of PvLb*a*, GmLb*a* and GmLbc_1 during natural and nitrate-induced senescence of nodules.

Y, young nodules; M, mature nodules; S, senescent nodules; 4N, young nodules after 4 days of NO_3^- treatment. Data are given as percentage of NO_2-Tyr^{30} relative to Tyr^{30}, and represent the mean ± SE of two or three biological replicates corresponding to different protein preparations. Asterisks denote statistical differences relative to young nodules at $P<0.05$ based on the Student's *t*-test. No differences in the NO_2-Tyr^{30} content of PvLb*a* were found in nodules treated with NO_3^- for 1, 2 or 3 days relative to untreated (control) nodules.

Figure 5. Molecular model of GmLb*a* showing the three Tyr residues.

(a) Positions of Tyr^{25}, Tyr^{30} and Tyr^{133} in relation to the heme.

(b) Tyr^{30} located in the distal heme pocket.

(c) Tyr^{133} in the edge of the heme, showing in both cases the distance between the Tyr hydroxyl and the oxoferryl. The GmLb*a* crystal structure (PDB accession 1BIN) was used for modeling with PyMOL software (www.pmol.org).

Figure 6. *In vitro* nitration of Lb.

(a) PvLb*a* (10 μM) was treated with H_2O_2 (100 μM) + NO_2^- (1 mM), then immediately loaded on SDS-gels, blotted and probed with anti-NO_2-Tyr antibody. (C+) positive control with complete mix. (C-) negative control omitting H_2O_2. Concentrations of compounds (added to the proteins before inclusion of H_2O_2 + NO_2^-): 100 μM DTPA, DFO and uric acid; 5 mM pHPA; 10 mM KCN. Similar results were obtained for GmLb*a*.

(b) Effect of SIN-1 on GmLb*a* and PvLb*a* nitration. The asterisk is a positive control of nitrated iron-superoxide dismutase (1 μg; Castro *et al.,* 2004). Numbers are the concentrations of SIN-1 (0.2-1 mM) and Lb (10-20 μM) used for the reactions and the amounts of Lb protein (3-6 μg) loaded per lane.

(c) Effect of $ONOO^-$ on GmLb*a* and PvLb*a* nitration. Lbs were treated with 500 μM $ONOO^-$ + HCO_3^- (5 mM) + DTPA (100 μM) for 5 min. Numbers are the concentrations of Lb (10-60 μM) used for the reactions and the amounts of Lb protein (3-6 μg) loaded per lane. Symbols +/- indicate addition or omission of $ONOO^-$. In panels (a) and (b), arrows mark the position of the monomeric Lbs. In panels (a) and (c), immunoreactive protein bands with molecular masses >27 kDa correspond to dimers and aggregates of nitrated Lb. For all panels, experiments were performed in 20 mM potassium phosphate buffer (pH 6.5) at 26°C, and molecular mass (kDa) markers are shown to the left.

Figure 7. Preparative separation and immunoblot analysis of Lb derivatives generated by nitration.

(a) Separation of Lb derivatives on preparative native gels. PvLb*a* (*upper gels*) and GmLb*a* (*lower gels*), both at 1 mM, were treated for 30 min with 10 mM H_2O_2 + 10 or 100 mM NO_2^- in 20 mM potassium phosphate buffer (pH 6.5). The protein products (bean, B1 to B7; soybean, S1 to S7) were eluted from gels and analyzed by MS.

(b) Immunoblot analyses of proteins eluted from (a) using antibodies against NO_2-Tyr and Lb. Besides monomeric nitrated Lb, dimers and other Lb aggregates (>27 kDa) were formed with different levels of nitration. GmLb*a* was more resilient to nitration than PvLb*a*, as the former showed less intense signal with the NO_2-Tyr antibody and maintained most Lb in monomeric form.

Figure 8. Mechanisms of protein Tyr nitration.

(a) Nitration mediated by ferryl globin (Glb^{4+}=O), which oxidizes NO_2^- to $\bullet NO_2$. The tyrosyl (•Tyr) radical cannot be generated directly from Tyr by reaction with H_2O_2 or $ONOO^-$ and its formation is very slow with $\bullet NO_2$ (Radi, 2004).

(b) Iron-catalyzed Fenton reaction followed by •OH-mediated NO_2^- oxidation.

(c) Nitration mediated by $ONOO^-$ and/or its derived radicals $\bullet NO_2$, •OH and $CO_3^{-\bullet}$. The nitrating species are indicated within boxes. For further explanation see Discussion.

REFERENCES

Álvarez, M.N., Trujillo, M. and Radi, R. (2002) Peroxynitrite formation from biochemical and cellular fluxes of nitric oxide and superoxide. *Methods Enzymol.* **359,** 353-366.

Álvarez, C., Lozano-Juste, J., Romero, L.C., García, I., Gotor, C. and León, J. (2011) Inhibition of *Arabidopsis O*-acetylserine(thiol)lyase A1 by tyrosine nitration. *J. Biol. Chem.* **286,** 578-586.

Appleby, C.A. and Bergersen, F.J. (1980) Preparation and experimental use of leghaemoglobin. In *Methods for Evaluating Biological Nitrogen Fixation* (Bergersen, F.J., ed.). Chichester:Wiley, pp. 315-335.

Arrese-Igor, C., Gordon, A.J., Minchin, F.R. and Denison, R.F. (1998) Nitrate entry and nitrite formation in the infected region of soybean nodules. *J. Exp. Bot.* **49,** 41-48.

Aviram, I., Wittenberg, B.A. and Wittenberg, J.B. (1978) The reaction of ferrous leghemoglobin with hydrogen peroxide to form leghemoglobin (IV). *J. Biol. Chem.* **253,** 5685-5689.

Balanbali, B., Kamisaki, Y., Martin, E. and Murad, F. (1999) Requirements for heme and thiols for the nonezymatic modification of nitrotyrosine. *Proc. Natl. Acad. Sci. USA* **96,** 13136-13141.

Bartesaghi, S., Trujillo, M., Denicola, A., Folkes, L., Wardman, P. and Radi, R. (2004) Reactions of desferrioxamine with peroxynitrite-derived carbonate and

nitrogen dioxide radicals. *Free Radic. Biol. Med.* **36,** 471-483.

Bartesaghi, S., Valez, V., Trujillo, M., Peluffo, G., Romero, N., Zhang, H., Kalyanaraman, B. and Radi, R. (2006) Mechanistic studies of peroxynitrite-mediated tyrosine nitration in membranes using the hydrophobic probe *N*-*t*-BOC-L-tyrosine *tert*-butyl ester. *Biochemistry* **45,** 6813-6825.

Becana, M., Minchin, F.R. and Sprent, J.I. (1989) Short-term inhibition of legume N_2 fixation by nitrate. I. Nitrate effects on nitrate-reductase activities of bacteroids and nodule cytosol. *Planta* **180,** 40-45.

Becana, M. and Klucas, R.V. (1992) Oxidation and reduction of leghemoglobin in root nodules of leguminous plants. *Plant Physiol.* **98,** 1217-1221.

Becana, M., Matamoros, M.A., Udvardi, M. and Dalton, D.A. (2010) Recent insights into antioxidant defenses of legume root nodules. *New Phytol.* **188,** 960-976.

Begara-Morales, J.C., Chaki, M., Sánchez-Calvo, B., Mata-Pérez, C., Leterrier, M., Palma, J.M., Barroso, J.B. and Corpas, F.J. (2013) Protein tyrosine nitration in pea roots during development and senescence. *J. Exp. Bot.* **64,** 1121-1134.

Bondoc, L.L. and Timkovich, R. (1989) Structural characterization of nitrimyoglobin. *J. Biol. Chem.* **264,** 6134-6145.

Castro, L., Eiserich, J.P., Sweeney, S., Radi, R. and Freeman, B.A. (2004) Cytochrome *c*: a catalyst and target of nitrite-hydrogen peroxide-dependent protein nitration. *Arch. Biochem. Biophys.* **421,** 99-107.

Cecconi, D., Orzetti, S., Vandelle, E., Rinalducci, S., Zolla, L. and Delledonne, M. (2009) Protein nitration during defense response in *Arabidopsis thaliana*. *Electrophoresis* **30,** 2460-2468.

Chaki, M., Valderrama, R., Fernández-Ocaña, A.M., Carreras, A., Gómez-Rodríguez, M.V., López-Jaramillo, J., Begara-Morales, J.C., Sánchez-Calvo, B., Luque, F., Leterrier, M., Corpas, F.J. and Barroso, J.B. (2011) High temperature triggers the metabolism of *S*-nitrosothiols in sunflower mediating a process of nitrosative stress which provokes the inhibition of ferredoxin-NADP reductase by tyrosine nitration. *Plant Cell Environ.* **34,** 1803-1818.

Corpas, F.J., del Río, L.A. and Barroso, J.B. (2007) Need of biomarkers of nitrosative stress in plants. *Trends Plant Sci.* **12,** 436-438.

Cueto, M., Hernández-Perera, O,. Martín, R., Bentura, M.L., Rodrigo, J., Lamas, S.

and Golvano, M.P. (1996) Presence of nitric oxide synthase activity in roots and nodules of *Lupinus albus*. *FEBS Lett.* **398,** 159-164.

Egelhofer, V., Hoehenwarter, W., Lyon, D., Weckwerth, W. and Wienkoop, S. (2013) Using ProtMAX to create high-mass-accuracy precursor alignments from label-free quantitative mass spectrometry data generated in shotgun proteomics experiments. *Nature Protocols* **8,** 595–601.

Escuredo, P.R., Minchin, F.R., Gogorcena, Y., Iturbe-Ormaetxe, I., Klucas, R.V. and Becana, M. (1996) Involvement of activated oxygen in nitrate-induced senescence of pea root nodules. *Plant Physiol.* **110,** 1187-1195.

Evans, P.J., Gallesi, D., Mathieu, C., Hernández, M.J., de Felipe, M.R., Halliwell, B. and Puppo, A. (1999) Oxidative stress occurs during soybean nodule senescence. *Planta* **208,** 73-79.

Fuchsman, W.H. and Appleby, C.A. (1979) Separation and determination of the relative concentrations of the homogenous components of soybean leghemoglobin by isoelectric focusing. *Biochim. Biophys. Acta* **579,** 314-324.

Galetskiy, D., Lohscheider, J.N., Kononikhin, A.S., Popov, I.A., Nikolaev, E.N. and Adamska, I. (2011) Phosphorylation and nitration levels of photosynthetic proteins are conversely regulated by light stress. *Plant Mol. Biol.* **77,** 461-473.

Gogorcena, Y., Gordon, A.J., Escuredo, P.R., Minchin, F.R., Witty, J.F., Moran, J.F. and Becana, M. (1997) N_2 fixation, carbon metabolism, and oxidative damage in nodules of dark-stressed common bean plants. *Plant Physiol.* **113,** 1193-1201.

Gow, A., Duran, D., Thom, S.R. and Ischiropoulos, H. (1996) Carbon dioxide enhancement of peroxynitrite-mediated protein tyrosine nitration. *Arch. Biochem. Biophys.* **333,** 42-48.

Herold, S. (2004) Nitrotyrosine, dityrosine, and nitrotryptophan formation from metmyoglobin, hydrogen peroxide, and nitrite. *Free Radic. Biol. Med.* **36,** 565-579.

Herold, S. and Puppo, A. (2005a) Oxyleghemoglobin scavenges nitrogen monoxide and peroxynitrite: a possible role in functioning nodules? *J. Biol. Inorg. Chem.* **10,** 935-945.

Herold, S. and Puppo, A. (2005b) Kinetics and mechanistic studies of the reactions of metleghemoglobin, ferrylleghemoglobin, and nitrosylleghemoglobin with reactive nitrogen species. *J. Biol. Inorg. Chem.* **10,** 946-957.

Herold, S. and Shivashankar, K. (2003) Metmyoglobin and methemoglobin catalyze the isomerization of peroxynitrite to nitrate. *Biochemistry* **42,** 14036-14046.

Jun, H.K., Sarath, G., Moran, J.F., Becana, M., Klucas, R.V. and Wagner, F.W. (1994) Characteristics of modified leghemoglobins isolated from soybean (*Glycine max* Merr.) root nodules. *Plant Physiol.* **104,** 1231-1236.

Kundu, S., Blouin, G.C., Premer, S.A., Sarath, G., Olson, J.S. and Hargrove, M.S. (2004) Tyrosine B10 inhibits stabilization of bound carbon monoxide and oxygen in soybean leghemoglobin. *Biochemistry* **43,** 6241-6252.

Lee, K.K., Shearman, L., Erickson, B.K. and Klucas, R.V. (1995) Ferric leghemoglobin in plant-attached leguminous nodules. *Plant Physiol.* **109,** 261-267.

Lozano-Juste, J., Colom-Moreno, R. and León, J. (2011) *In vivo* protein tyrosine nitration in *Arabidopsis thaliana*. *J. Exp. Bot.* **62,** 3501-3517.

Mathieu, C., Moreau, S., Frendo, P., Puppo, A. and Davies, M.J. (1998) Direct detection of radicals in intact soybean nodules: presence of nitric oxide leghemoglobin complexes. *Free Radic. Biol. Med.* **24,** 1242-1249.

Meakin, G.E., Bueno, E., Jepson, B., Bedmar, E.J., Richardson, D.J. and Delgado, M.J. (2007) The contribution of bacteroidal nitrate and nitrite reduction to the formation of nitrosylleghaemoglobin complexes in soybean root nodules. *Microbiology* **153,** 411-419.

Melo, P.M., Silva, L.S., Ribeiro, I., Seabra, A.R. and Carvalho, H.G. (2011) Glutamine synthetase is a molecular target of nitric oxide in root nodules of *Medicago truncatula* and is regulated by tyrosine nitration. *Plant Physiol.* **157,** 1505-1517.

Moreau, S., Davies, M.J. and Puppo, A. (1995) Reaction of ferric leghemoglobin with H_2O_2: formation of heme-protein cross-links and dimeric species. *Biochim. Biophys. Acta* **1251,** 17-22.

Moreau, S., Davies, M.J., Mathieu, D., Hérouart, D. and Puppo, A. (1996) Leghemoglobin-derived radicals. Evidence for multiple protein-derived radicals and the initiation of peribacteroid membrane damage. *J. Biol. Chem.* **271,** 32557-32562.

Navascués, J., Pérez-Rontomé, C., Gay, M., Marcos, M., Yang, F., Walker, F.A., Desbois, A., Abián, J. and Becana, M. (2012) Leghemoglobin green derivatives with nitrated hemes evidence production of highly reactive nitrogen species during

aging of legume nodules. *Proc. Natl. Acad. Sci. USA* **109,** 2660-2665.

Nicolis, S., Monzani, E., Roncone, R., Gianelli, L. and Casella, L. (2004) Metmyoglobin-catalyzed exogenous and endogenous tyrosine nitration by nitrite and hydrogen peroxide. *Chem. Eur. J.* **10,** 2281-2290.

Otsuka, M., Marks, S.A., Winnica, D.E., Amoscato, A.A., Pearce, L.L. and Peterson, J. (2010) Covalent modifications of hemoglobin by nitrite anion: formation kinetics and properties of nitrihemoglobin. *Chem. Res. Toxicol.* **23,** 1786-1795.

Petruk, A.A., Bartesaghi, S., Trujillo, M., Estrin, D.A., Murgida, D., Kalyanaraman, B., Marti, M.A. and Radi, R. (2012) Molecular basis of intramolecular electron transfer in proteins during radical-mediated oxidations: computer simulation studies in model tyrosine-cysteine peptides in solution. *Arch. Biochem. Biophys.* **525,** 82-91.

Pfeiffer, N.E., Torres, C.M. and Wagner, F.W. (1983) Proteolytic activity in soybean root nodules. Activity in host cell cytosol and bacteroids throughout physiological development and senescence. *Plant Physiol.* **71,** 797-802.

Pladys, D., Barthe, P. and Rigaud, J. (1988) Changes in intracellular pH in French-bean nodules induced by senescence and nitrate treatment. *Plant Sci.* **56,** 99-106.

Prasad, J.C., Goldstone, J.V., Camacho, C.J., Vajda, S. and Stegeman, J.J. (2007) Ensemble modeling of substrate binding to cytochromes P450: analysis of catalytic differences between CYP1A orthologs. *Biochemistry* **46,** 2640-2654.

Puppo, A., Groten, K., Bastian, F., Carzaniga, R., Soussi, M., Lucas, M.M., de Felipe, M.R., Harrison, J., Vanacker, H. and Foyer, C.H. (2005) Legume nodule senescence: roles for redox and hormone signalling in the orchestration of the natural aging process. *New Phytol.* **165,** 683-701.

Radi, R. (2004) Nitric oxide, oxidants, and protein tyrosine nitration. *Proc. Natl. Acad. Sci. USA* **101,** 4003-4008.

Sakamoto, A., Sakurao, S.H., Fukunaga, K., Matsubara, T., Ueda-Hashimoto, M., Tsukamoto, S., Takahashi, M. and Morikawa, H. (2004) Three distinct *Arabidopsis* hemoglobins exhibit peroxidase-like activity and differentially mediate nitrite-dependent protein nitration. *FEBS Lett.* **572,** 27-32.

Schopfer, F.J., Baker, P.R.S. and Freeman, B.A. (2003) NO-dependent protein nitration: a cell signaling event or an oxidative inflammatory response? *Trends Biochem. Sci.* **28,** 646-654.

Söderling, A., Hultman, L., Delbro, D., Højrup, P. and Caidahl, K. (2007) Reduction of the nitro group during sample preparation may cause underestimation of the nitration level in 3-nitrotyrosine immunoblotting. *J. Chromatography B* **851,** 277-286.

Tanou, G., Filippou, P., Belghazi, M., Job, D., Diamantidis, G., Fotopoulos, V. and Molassiotis, A. (2012) Oxidative and nitrosative-based signaling and associated post-translational modifications orchestrate the acclimation of citrus plants to salinity stress. *Plant J.* **72,** 585-599.

Thomas, D.D., Espey, M.G., Vitek, M.P., Miranda, K.M. and Wink, D.A. (2002) Protein nitration is mediated by heme and free metals through Fenton-type chemistry: an alternative to the NO/O_2^- reaction. *Proc. Natl. Acad. Sci. USA* **99,** 12691-12696.

Van der Vliet, A., Eiserich, J.P., Halliwell, B. and Cross, C.E. (1997) Formation of reactive nitrogen species during peroxidase-catalyzed oxidation of nitrite. *J. Biol. Chem.* **272,** 7617-7625.

Table 1 *In vitro* nitration of Tyr residues of Lbs

Lb[a]	Tyr	% Nitration[b]	
		0.1 mM H_2O_2 + 0.1 mM NO_2^-	**0.1 mM H_2O_2 + 1 mM NO_2^-**
PvLb*a*	Tyr^{25}	0.4	1.4
	Tyr^{30}	54.4	75.9
GmLb*a*	Tyr^{25}	0.6	1.1
	Tyr^{30}	49.9	77.7
GmLbc_1	Tyr^{25}	13.5	0.9
	Tyr^{30}	25.3	64.4
GmLbc_2	Tyr^{25}	0.5	0.6
	Tyr^{30}	38.3	65.6
GmLbc_3	Tyr^{25}	0.5	0.4
	Tyr^{30}	32.1	55.2

[a] All Lbs were used at a concentration of 10 μM.
[b] Percentage of nitration = [NO_2-Tyr/(NO_2-Tyr + Tyr)] x 100. Values are means of two or three biological replicates with SE<10%.

Figure 1

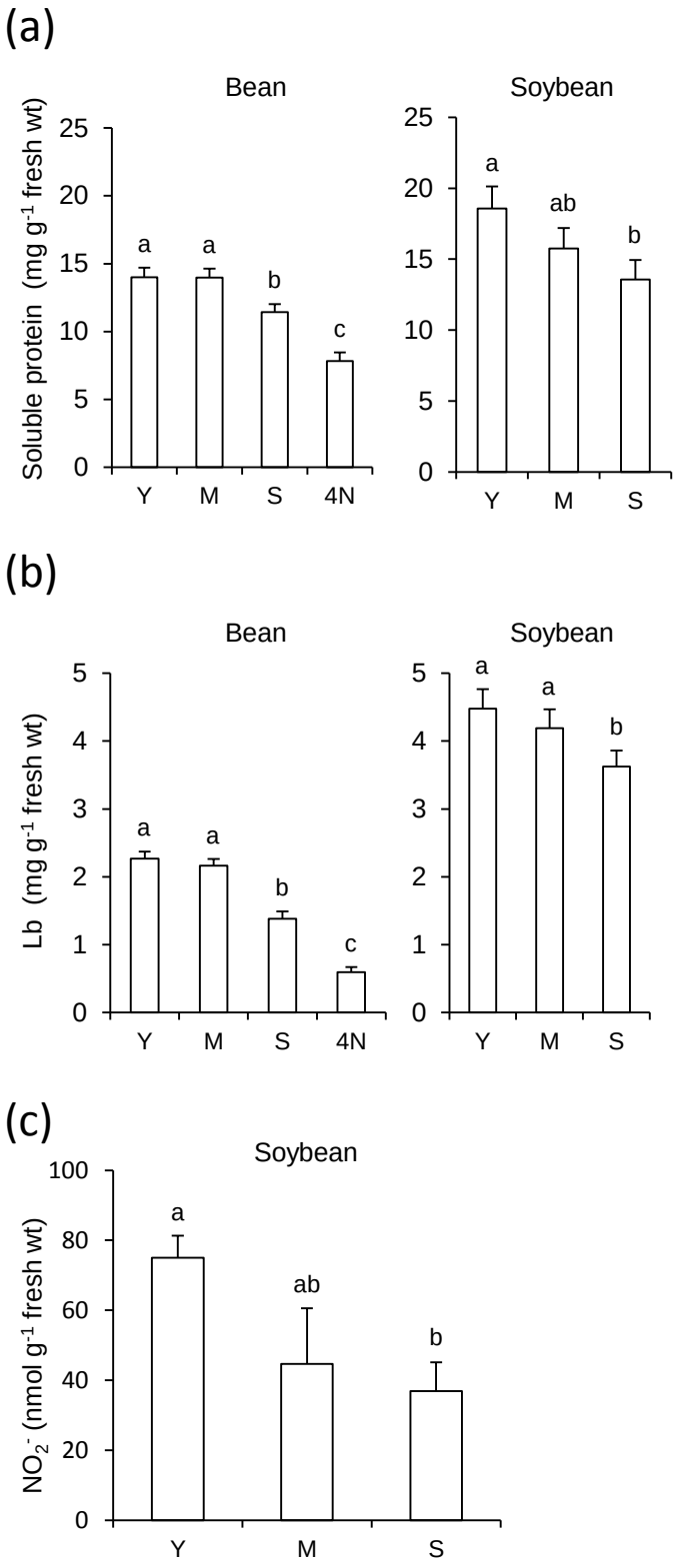
(a)
Bean
Soybean
Soluble protein (mg g-1 fresh wt)
25
20
15
10
5
0
a
a
b
c
ab
Y
M
S
4N
(b)
Lb (mg g-1 fresh wt)
4
3
2
1
(c)
NO2- (nmol g-1 fresh wt)
100
80
60
40
20

Figure 2

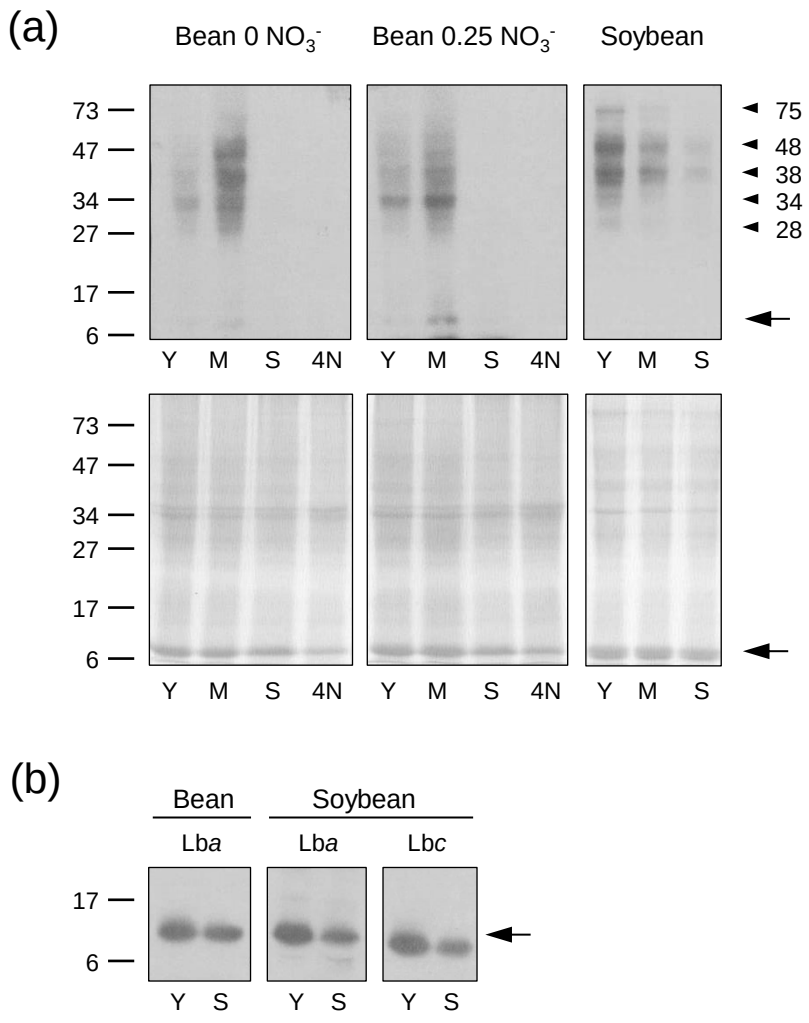
(a)
Bean 0 NO3-
Bean 0.25 NO3-
Soybean
73
47
34
27
17
6
75
48
38
34
28
Y M S 4N Y M S 4N Y M S
Y M S 4N Y M S 4N Y M S
(b)
Bean
Soybean
Lba
Lba
Lbc
17
6
Y S Y S Y S

Figure 3

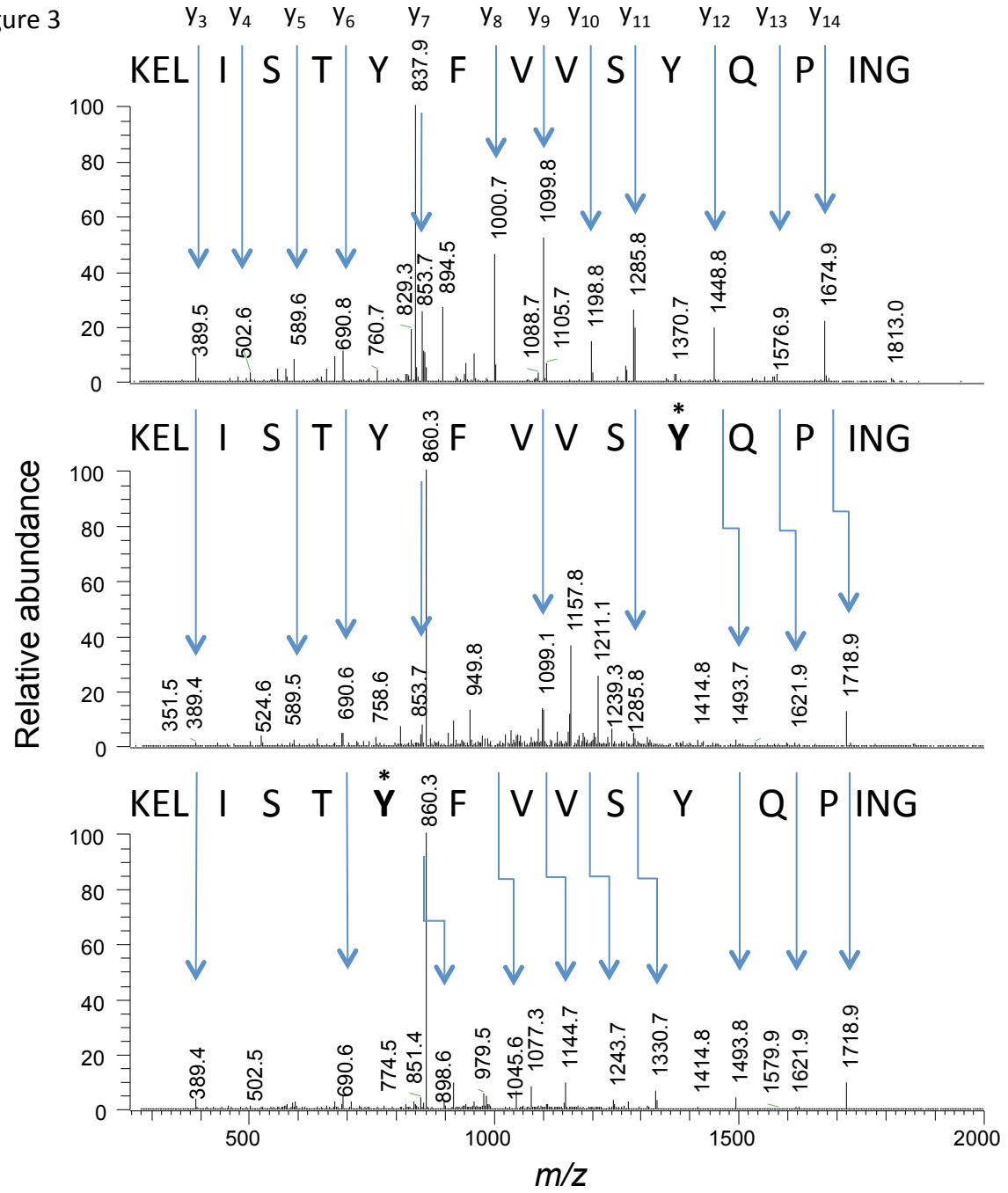

NL: 1.04E7
ms2 979.50, cid35.00

GNIPQYSVVFYTSILEK
not nitrated

NL: 1.21E4
ms2 1002.00, cid35.00

GNIPQ**Y***SVVFYTSILEK
NO_2-Tyr^{25}

NL: 3.09E4
ms2 1002.00, cid35.00

GNIPQYSVVF**Y***TSILEK
NO_2-Tyr^{30}

Figure 4

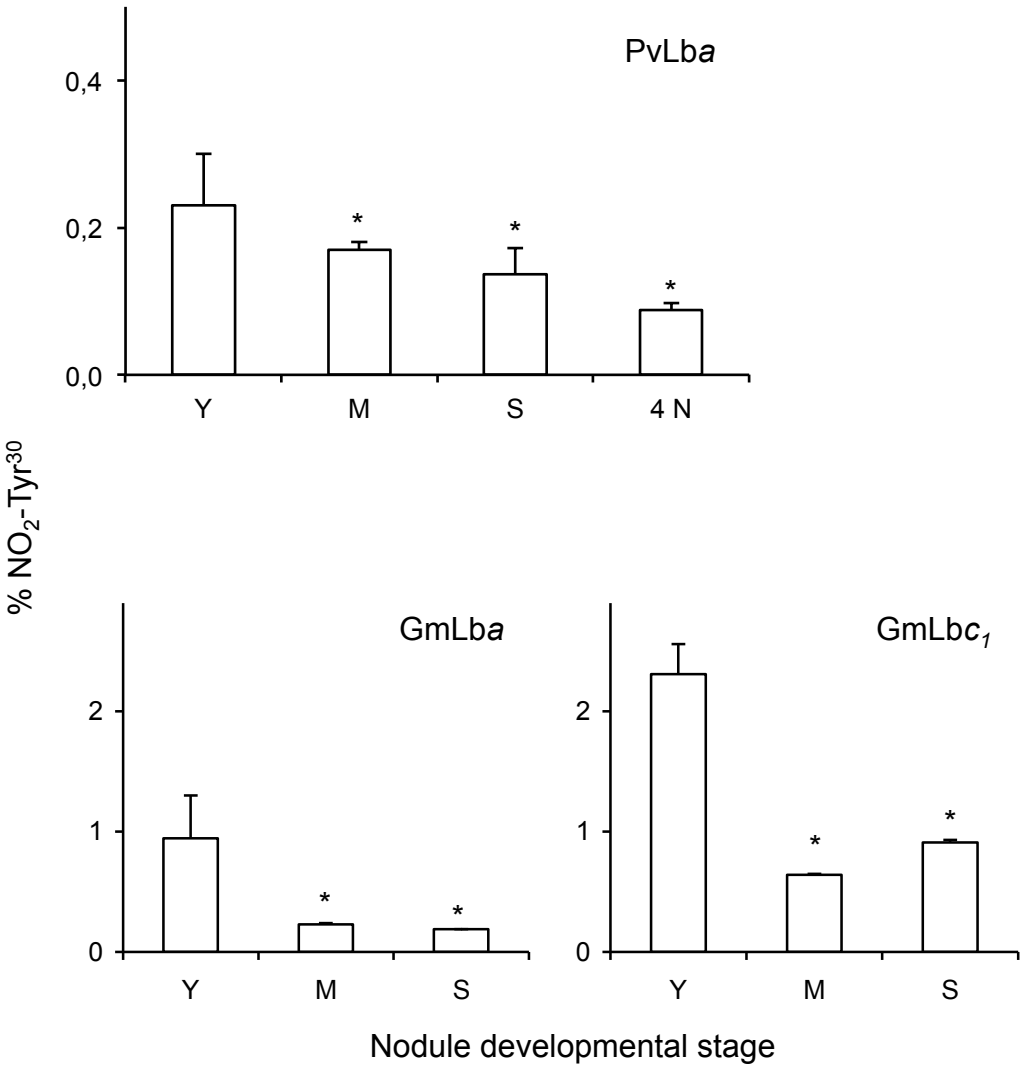
PvLba
0,4
0,2
0,0
Y
M
S
4 N
% NO2-Tyr30
GmLba
GmLbc1
2
1
0
Y
M
S
Nodule developmental stage

Figure 5

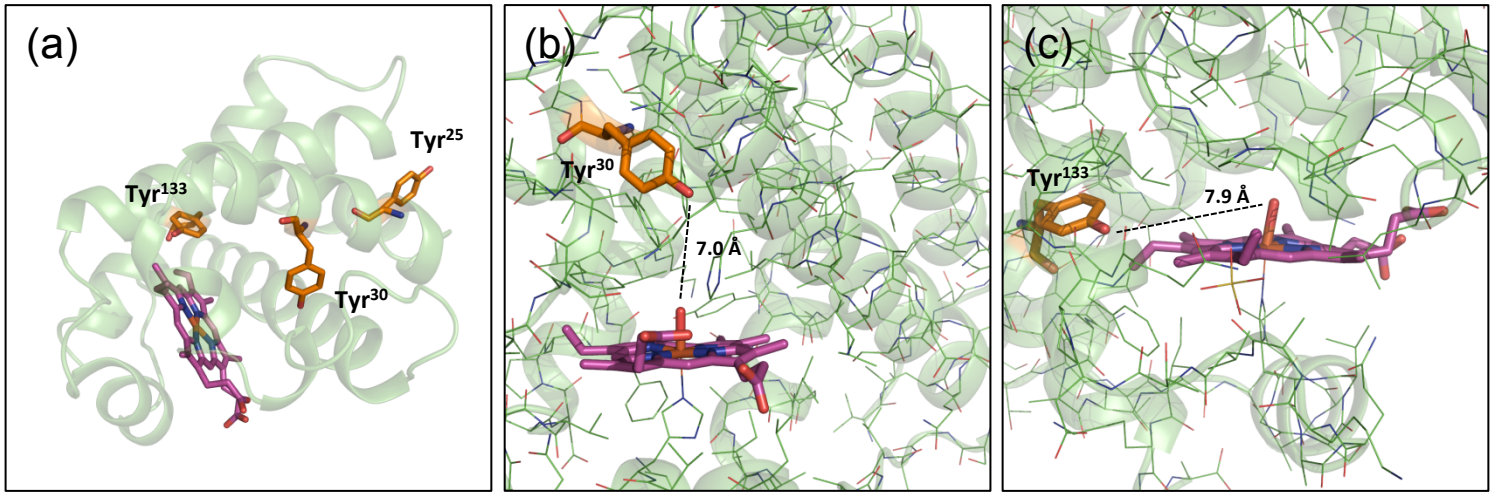

Figure 6

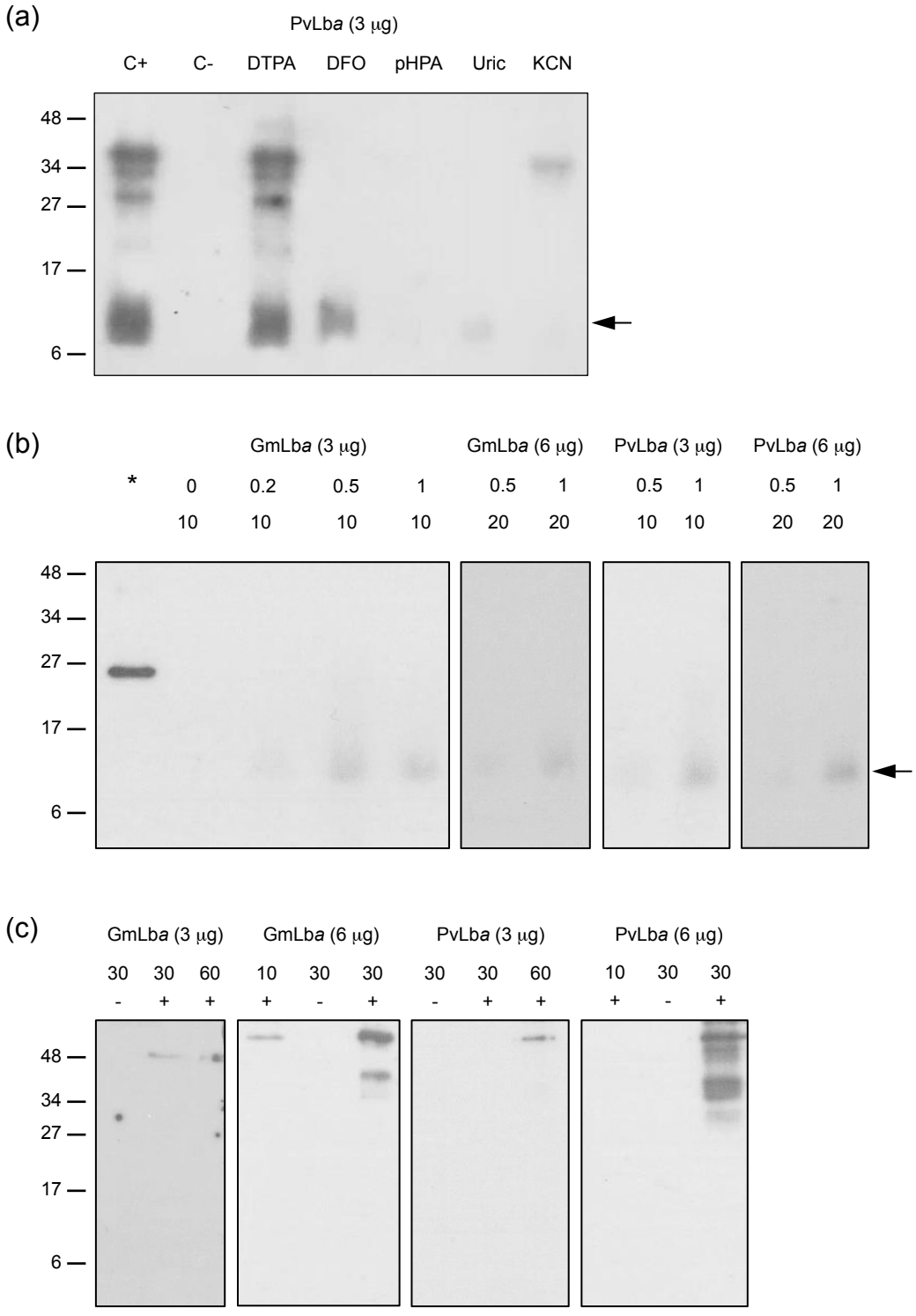
(a)
PvLba (3 μg)
C+
C-
DTPA
DFO
pHPA
Uric
KCN
48
34
27
17
6
(b)
GmLba (3 μg)
GmLba (6 μg)
PvLba (3 μg)
PvLba (6 μg)
*
0
0.2
0.5
1
0.5
1
0.5
1
0.5
1
10
10
10
10
20
20
10
10
20
20
48
34
27
17
6
(c)
GmLba (3 μg)
GmLba (6 μg)
PvLba (3 μg)
PvLba (6 μg)
30 30 60
10 30 30
30 30 60
10 30 30
- + +
+ - +
- + +
+ - +
48
34
27
17
6

Figure 7

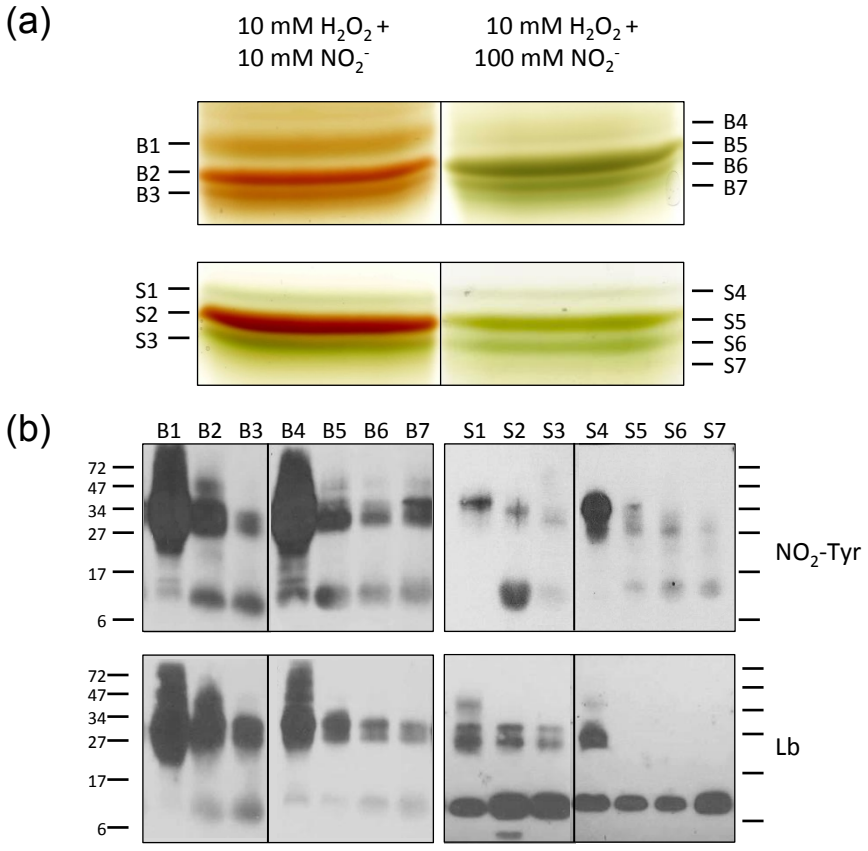
(a)
10 mM H_2O_2 + 10 mM NO_2^-
10 mM H_2O_2 + 100 mM NO_2^-
B1
B2
B3
B4
B5
B6
B7
S1
S2
S3
S4
S5
S6
S7
(b)
B1 B2 B3 B4 B5 B6 B7 S1 S2 S3 S4 S5 S6 S7
72
47
34
27
17
6
NO_2-Tyr
Lb

Figure 8

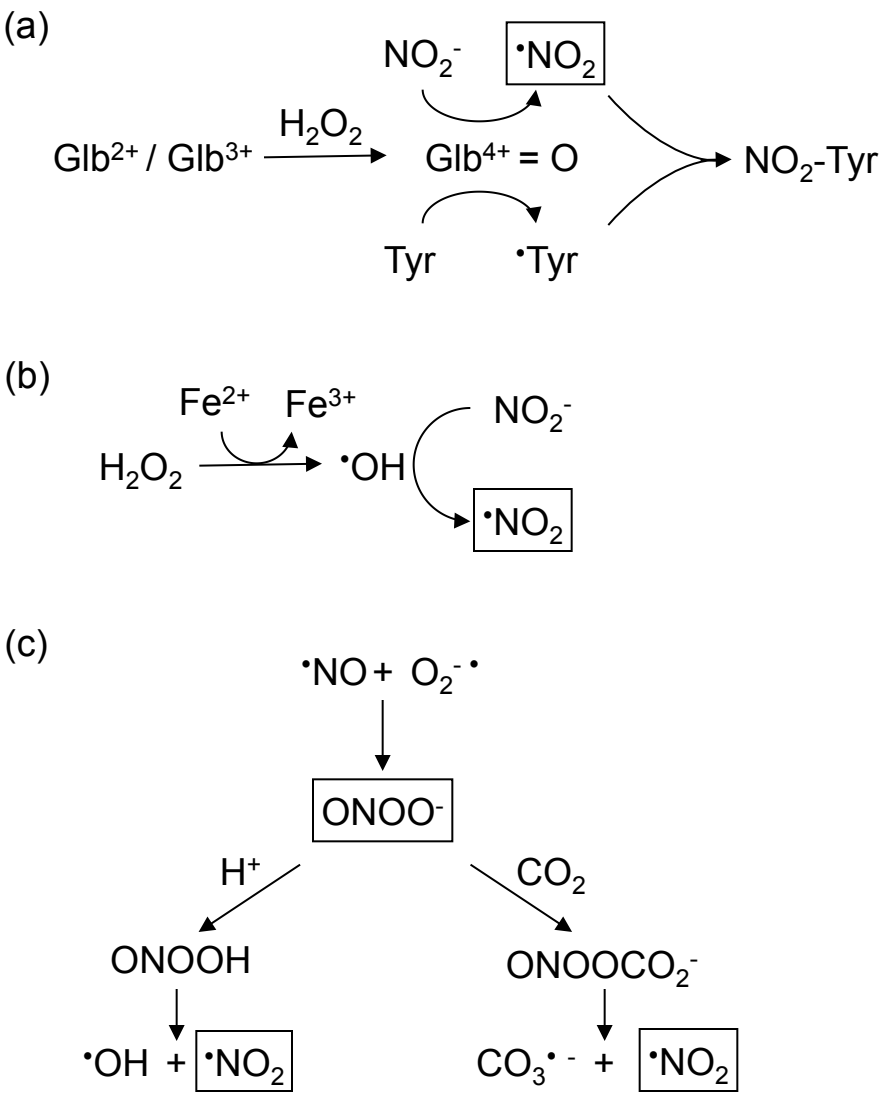
(a)
NO_2^-
$^{\bullet}NO_2$
H_2O_2
Glb^{2+} / Glb^{3+}
Glb^{4+} = O
NO_2-Tyr
Tyr
$^{\bullet}$Tyr
(b)
Fe^{2+}
Fe^{3+}
NO_2^-
H_2O_2
$^{\bullet}OH$
$^{\bullet}NO_2$
(c)
$^{\bullet}NO$ + $O_2^{-\bullet}$
$ONOO^-$
H^+
CO_2
ONOOH
$ONOOCO_2^-$
$^{\bullet}OH$ + $^{\bullet}NO_2$
$CO_3^{\bullet -}$ + $^{\bullet}NO_2$

Table S1 Compilation of data obtained for Lb derivatives using immunoblots, low-resolution MS and high-resolution MS

Protein[a]	Color	Nitrated monomer[b]	Nitrated dimer[b]	Nitrated aggregate[b]	Nitrated heme[c]	Molecular masses[d]
B1	Red	+	+	+	+	15243, 15290, 15492
B2	Red	+	+	+	+	15245, 15290, 15524
B3	Red	+	+	-	+	15289, 15523, 15568
B4	Green	+	+	+	+	15289, 15524, 15569
B5	Green	+	+	+/-	-	15289
B6	Green	+	+	+/-	+/-	15290
B7	Green	+	+	+/-	+/-	15289
S1	Green	+	+	-	-	15278
S2	Red	+	+	-	+	15278
S3	Green	+	+	-	+	15278
S4	Green	+	+	-	-	15278, 15881
S5	Green	+	+	-	-	15278
S6	Green	+	+	-	+/-	15278
S7	Green	+	+	-	+/-	15278, 15881

[a] Designation of protein bands as shown in Figure 6.
[b] Nitrated Lbs in monomeric, dimeric, or aggregated forms. (+) present at significant amounts based on immunoblots and/or MS analyses; (-) absent; or (+/-) present at very low amounts.
[c] Heme with molecular ion of *m/z* 661. Symbols as in the footnote above.
[d] Molecular masses other than those of the unmodified (control) proteins (15479 for bean Lb*a* and15233 for soybean Lb*a*). Identified nitrated proteins are marked in red. Note the presence of mononitrated Lbs (15524 for bean and15278 for soybean) and dinitrated Lbs (15569 for bean).

Table S2 MS/MS transitions monitored for the calculation of the nitration ratio. Ratios were calculated taking into account the areas of two or three of the major product ions in the fragmentation spectrum for each peptide

Proteins and peptides[a]	*m/z* precursor ion	*m/z* monitored fragments > fragment type		
PvLb*a* *(P02234)*				
GNIPQ**Y**SVVF**Y**TSILEK	1024.50	882.43 > y14(2+)	1144.59 > y9(1+)	690.40 > y6(1+)
GNIPQ**Y**SVVFYTSILEK	1002.01	859.93 > y14(2+)	1099.60 > y9(1+)	690.40 > y6(1+)
GNIPQYSVVF**Y**TSILEK	1002.01	859.93 > y14(2+)	1144.59 > y9(1+)	690.40 > y6(1+)
GNIPQYSVVFYTSILEK	979.52	837.44 > y14(2+)	1099.60 > y9(1+)	690.40 > y6(1+)
WTDELSTALELAYDELAAAIK	1162.09	993.53 > y9(1+)	715.43 > y7(1+)	
WTDELSTALELA**Y**DELAAAIK	1184.58	993.53 > y9(1+)	1038.52 > y7(1+)	
GmLb*a* *(P02238)*				
ANIPQ**Y**SVVF**Y**NSILEK	1031.51	882.43 > y14(2+)	1144.59 > y9(1+)	690.40 > y6(1+)
ANIPQ**Y**SVVFYNSILEK	1009.02	859.94 > y14(2+)	1099.60 > y9(1+)	690.40 > y6(1+)
ANIPQYSVVF**Y**NSILEK	1009.02	859.94 > y14(2+)	1144.59 > y9(1+)	690.40 > y6(1+)
ANIPQYSVVFYNSILEK	986.52	837.44 > y14(2+)	1099.60 > y9(1+)	690.40 > y6(1+)
AWEVAYDELAAAIK	775.40	993.53 > y9(1+)	830.46 > y8(1+)	
AWEVA**Y**DELAAAIK	797.89	1038.51 > y9(1+)	830.46 > y8(1+)	
GmLb*c1* *(P02235)*				
ANIPQ**Y**SVVF**Y**TSILEK	1038.01	888.93 > y14(2+)	1157.58 > y9(1+)	703.40 > y6(1+)
ANIPQ**Y**SVVFYTSILEK	1015.52	866.43 > y14(2+)	1112.63 > y9(1+)	703.40 > y6(1+)
ANIPQYSVVF**Y**TSILEK	1015.52	866.43 > y14(2+)	1157.58 > y9(1+)	703.40 > y6(1+)
ANIPQYSVVFYTSILEK	993.02	843.94 > y14(2+)	1112.60 > y9(1+)	703.40 > y6(1+)
EAVGGNWSDELSSAWEVAYDELAAAIK	1441.18	1064.56 > y10(2+)	830.46 > y8(1+)	
EAVGGNWSDELSSAWEVA**Y**DELAAAIK	1463.66	1109.52 > y10(2+)	830.46 > y8(1+)	
GmLb*c2* *(P02236)*				
ANIPQ**Y**SVVF**Y**NSILEK	1031.51	882.43 > y14(2+)	1144.59 > y9(1+)	690.40 > y6(1+)
ANIPQ**Y**SVVFYNSILEK	1009.02	859.93 > y14(2+)	1099.63 > y9(1+)	690.40 > y6(1+)
ANIPQYSVVF**Y**NSILEK	1009.02	859.93 > y14(2+)	1144.59 > y9(1+)	690.40 > y6(1+)
ANIPQYSVVFYNSILEK	986.52	837.44 > y14(2+)	1099.60 > y9(1+)	690.40 > y6(1+)
WSDELSSAWEVAYDELAAAIK	1177.56	993.53 > y9(1+)	715.43 > y7(1+)	
WSDELSSAWEVA**Y**DELAAAIK	1200.04	1038.49 > y9(1+)	715.43 > y7(1+)	
GmLb*c3* *(P02237)*				
TNIPQ**Y**SVVF**Y**TSILEK	1046.52	882.43 > y14(2+)	1144.59 > y9(1+)	690.40 > y6(1+)
TNIPQ**Y**SVVFYTSILEK	1024.02	859.94 > y14(2+)	1099.63 > y9(1+)	690.40 > y6(1+)
TNIPQYSVVF**Y**TSILEK	1024.02	859.94 > y14(2+)	1144.59 > y9(1+)	690.40 > y6(1+)
TNIPQYSVVFYTSILEK	1001.53	837.44 > y14(2+)	1099.60 > y9(1+)	690.40 > y6(1+)
WSDELSSAWEVAYDELAAAIK	1177.56	993.53 > y9(1+)	715.43 > y7(1+)	
WSDELSSAWEVA**Y**DELAAAIK	1200.04	1038.49 > y9(1+)	715.43 > y7(1+)	

[a] UniProt accessions (UniRef100) are given in parentheses and NO_2-Tyr are indicated in boldface and red.

Figure S1

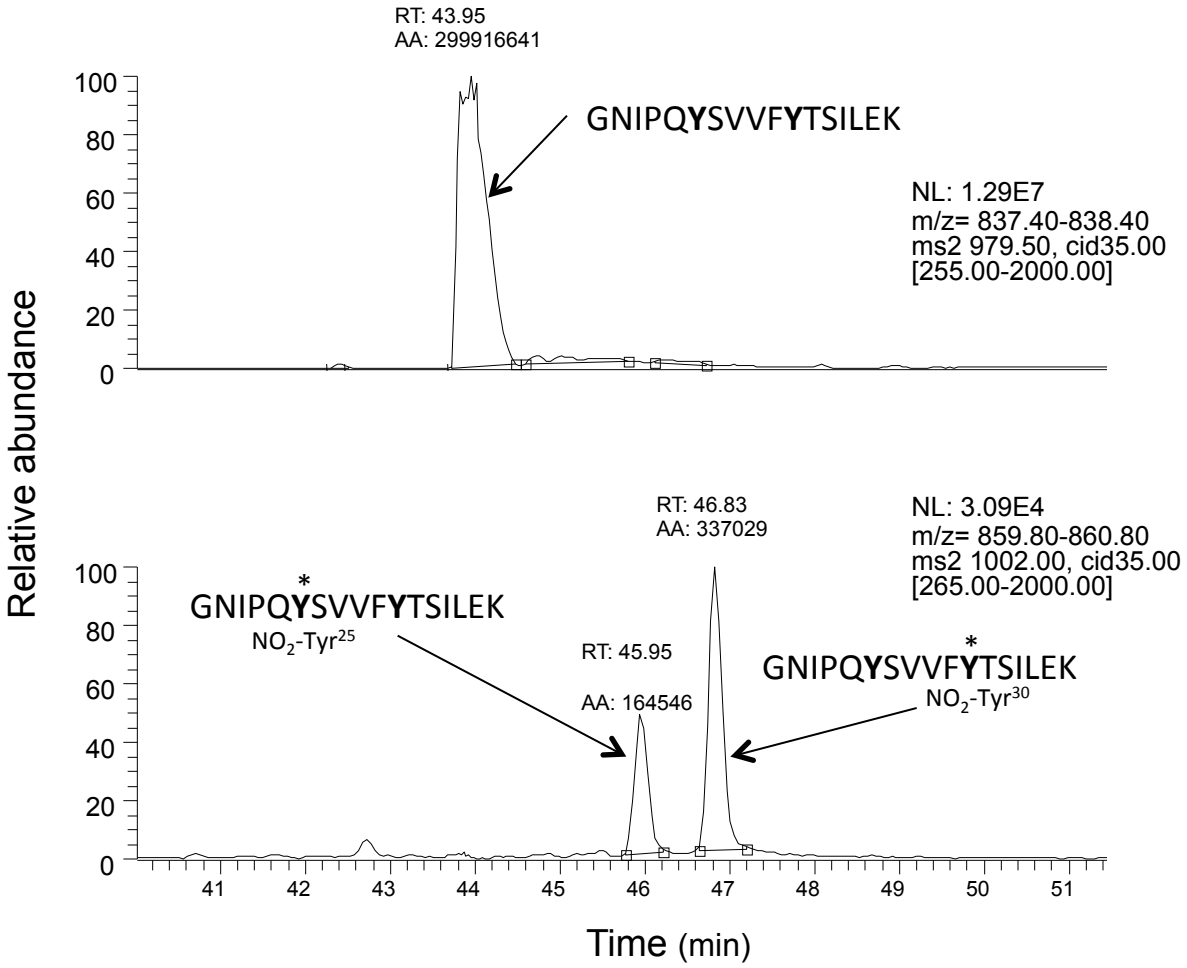
RT: 43.95
AA: 299916641
GNIPQ**Y**SVVF**Y**TSILEK
NL: 1.29E7
m/z= 837.40-838.40
ms2 979.50, cid35.00
[255.00-2000.00]
RT: 46.83
AA: 337029
NL: 3.09E4
m/z= 859.80-860.80
ms2 1002.00, cid35.00
[265.00-2000.00]
*
GNIPQ**Y**SVVF**Y**TSILEK
NO_2-Tyr^{25}
RT: 45.95
AA: 164546
*
GNIPQ**Y**SVVF**Y**TSILEK
NO_2-Tyr^{30}
Relative abundance
Time (min)

Figure S2

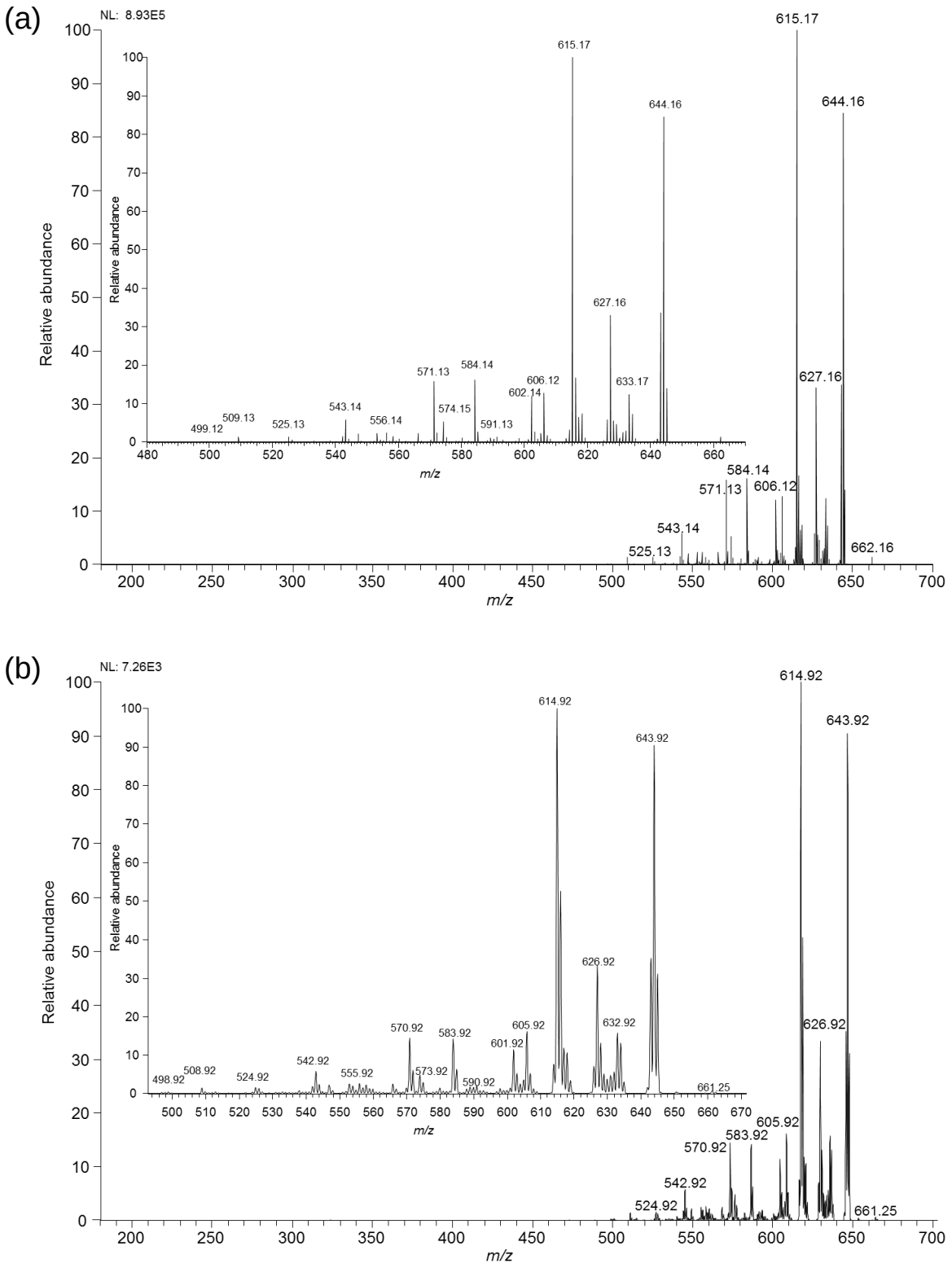
(a)
NL: 8.93E5
Relative abundance
m/z
615.17
644.16
627.16
584.14
571.13
606.12
543.14
525.13
662.16
(b)
NL: 7.26E3
Relative abundance
m/z
614.92
643.92
626.92
605.92
583.92
570.92
542.92
524.92
661.25